Molecular Microbiology (2011) 80(3), 596–611 ■
doi:10.1111/j.1365-2958.2011.07577.x
First published online 24 February 2011

# Biphasic control logic of HAMP domain signalling in the *Escherichia coli* serine chemoreceptor

**Qin Zhou, Peter Ames and John S. Parkinson***
*Biology Department, University of Utah, Salt Lake City, Utah 84112, USA*

## Summary

**HAMP domains mediate input–output communication in many bacterial signalling proteins. To explore the dynamic bundle model of HAMP signalling (Zhou *et al*., *Mol. Microbiol*. 73: 801, 2009), we characterized the signal outputs of 118 HAMP missense mutants of the serine chemoreceptor, Tsr, by flagellar rotation patterns. Receptors with proline or charged amino acid replacements at critical hydrophobic packing residues in the AS1 and AS2 HAMP helices had locked kinase-off outputs, indicating that drastic destabilization of the Tsr-HAMP bundle prevents kinase activation, both in the absence and presence of the sensory adaptation enzymes, CheB and CheR. Attractant-mimic lesions that enhance the structural stability of the HAMP bundle also suppressed kinase activity, demonstrating that Tsr-HAMP has two kinase-off output states at opposite extremes of its stability range. HAMP mutants with locked-on kinase outputs appeared to have intermediate bundle stabilities, implying a biphasic relationship between HAMP stability and kinase activity. Some Tsr-HAMP mutant receptors exhibited reversed output responses to CheB and CheR action that are readily explained by a biphasic control logic. The findings of this study provide strong support for a three-state dynamic bundle model of HAMP signalling in Tsr, and possibly in other bacterial transducers as well.**

## Introduction

Motile *Escherichia coli* cells track chemical gradients with high sensitivity over wide concentration ranges [recently reviewed in (Hazelbauer *et al*., 2008; Hazelbauer and Lai, 2010)]. Stimulus detection, amplification and integration occur in an arrayed network of signalling complexes that contain transmembrane chemoreceptors (methyl-accepting chemotaxis proteins or MCPs), the signalling histidine kinase CheA, and CheW, which couples CheA activity to chemoreceptor control. In the absence of chemoattractant gradients, MCPs activate CheA, promoting frequent episodes of clockwise (CW) flagellar rotation and random changes in swimming direction. Binding of an attractant ligand to the periplasmic sensing domain of a receptor molecule downregulates CheA bound to the cytoplasmic tip of the receptor, promoting counterclockwise (CCW) flagellar rotation and forward swimming (Fig. 1). A sensory adaptation system subsequently restores pre-stimulus behaviour through changes in MCP methylation state, catalysed by a dedicated methyltransferase (CheR) and methylesterase (CheB).

A 50-residue HAMP domain plays a key mechanistic role in transmembrane signalling by bacterial chemoreceptors. HAMP domains promote two-way conformational communication between the input and output domains of many bacterial signalling proteins, including sensor histidine kinases, adenylyl cyclases, MCPs and phosphatases (Aravind and Ponting, 1999; Williams and Stewart, 1999). HAMP subunits contain two amphiphilic helices (AS1, AS2) joined by a non-helical connector segment (CTR). These conserved structural elements probably organize into four-helix bundles in homodimeric signalling proteins (Butler and Falke, 1998; Swain and Falke, 2007; Watts *et al*., 2008), as suggested by several high-resolution HAMP structures (Hulko *et al*., 2006; Airola *et al*., 2010), by *in vitro* and *in vivo* receptor cross-linking studies (Swain and Falke, 2007; Watts *et al*., 2008), and by analyses of HAMP lesions in chemoreceptors (Ames *et al*., 2008; Zhou *et al*., 2009) and in sensor histidine kinases (Parkinson, 2010; Stewart and Chen, 2010).

Studies of *E. coli* chemoreceptors and sensor kinases demonstrate that HAMP domains can be locked in kinase-activating or kinase-inhibiting output states by mutational alterations and by cysteine-targeted disulfide bonds (Parkinson, 2010). The gearbox (Hulko *et al*., 2006) and scissors (Swain and Falke, 2007) models of HAMP signalling propose discrete kinase-on and kinase-off conformations that correspond to alternate packing arrangements or pivoting motions of the HAMP helices. In contrast, the dynamic bundle model proposes that HAMP signal state depends on the structural stability of the HAMP bundle

Accepted 29 January, 2011. *For correspondence. E-mail parkinson@biology.utah.edu; Tel. (801) 581-7639; Fax (801) 581 4668.

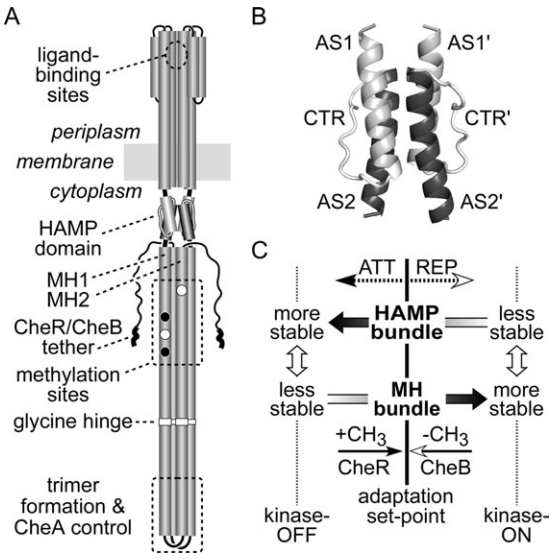


**Fig. 1.** Tsr and HAMP structure and our initial dynamic bundle signalling model.
A. Important signalling features of the Tsr dimer. Cylindrical segments represent α-helical regions, drawn approximately to scale. Methylation sites shown as black circles indicate glutamine residues that must be deamidated to glutamates by CheB before accepting methyl groups; open circles represent glutamate residues that are direct substrates for the CheR methyltransferase. Thickened regions at the C-terminus of each subunit represent a pentapeptide sequence (NWETF) to which CheB and CheR bind.
B. Probable structure of the HAMP domain in a Tsr dimer. Each HAMP subunit consists of two amphiphilic helices (AS1, AS2) joined by a non-helical connector (CTR). The four-helix bundle is modelled on the atomic co-ordinates for Af1503 HAMP (Hulko *et al*., 2006), as described (Ames *et al*., 2008). The four helices pack in parallel orientation (N-termini at the top). This grayscale shading convention for the HAMP structural elements is used in all subsequent figures.
C. Dynamic bundle model of HAMP signalling (Zhou *et al*., 2009). The original model proposed that chemoeffector stimuli control signal output by modulating the packing stability of the HAMP bundle, which is oppositionally coupled to the stability of the MH1/MH1' packing interactions. Methylation and demethylation of sites in the MH bundle shift stability in the opposing direction to reverse HAMP signalling effects during sensory adaptation.

and its adjoining output helices (Zhou *et al*., 2009) (Fig. 1C).

In the dynamic bundle model, the attractant-induced kinase-off state corresponds to a stable packing arrangement of the HAMP four-helix bundle (Zhou *et al*., 2009). The alternative, repellent-induced kinase-on state corresponds to a less stably packed, more dynamic HAMP bundle (Fig. 1C). A helical phase clash at the AS2-MH1 junction may produce an oppositional coupling of AS2/AS2' and MH1/MH1' packing stabilities: The four-helix MH bundle should be loosely packed in the attractant-induced kinase-off state and more stably packed in the repellent-induced kinase-on state (Fig. 1C). The sensory adaptation system may counteract HAMP control by also influencing the packing interactions of the methylation helices: CheR-mediated methylation enhances MH bundle stability; CheB-mediated demethylation, or deamidation of glutamines (Q) to glutamates (E) at potential methyl-accepting sites, reduces MH bundle stability (Starrett and Falke, 2005; Winston *et al*., 2005).

To explore the nature of HAMP output states in Tsr, the serine chemoreceptor, we characterized the signalling properties of Tsr molecules with HAMP amino acid replacements that abrogated signal transmission. Our results provide evidence for two kinase-off signalling states at opposite extremes of the HAMP stability range and a biphasic relationship between HAMP stability and kinase activity. Mutations that destabilize the HAMP bundle can drive the system to a variety of non-physiological states, including ones that lock output in high or low kinase activity or that produce reversed control responses to adaptational modifications. These findings provide strong support for a three-state dynamic bundle model of HAMP input–output control in chemoreceptors, and possibly in other HAMP-containing transducers as well.

## Results

### *Assessing receptor output and sensory adaptation with flagellar rotation patterns*

Receptors in a kinase-on signalling state enhance autophosphorylation of CheA, which in turn donates phosphoryl groups to the response regulators, CheB and CheY (Hess *et al*., 1988; Wylie *et al*., 1988; Borkovich *et al*., 1989; Borkovich and Simon, 1990). Phospho-CheY interacts with the switch complex at the base of flagellar motors to augment CW rotation (Smith *et al*., 1988; Barak and Eisenbach, 1992; Welch *et al*., 1993). Receptors that cannot activate CheA cannot produce phospho-CheY, resulting in CCW rotation of the flagellar motors, the default direction. Because the extent of CW rotation is directly related to CheA activity, flagellar rotation patterns reflect receptor signalling state: Kinase-off receptors produce CCW behaviour; kinase-on receptors produce CW behaviour. In the ensuing discussion, we often refer to receptor output signals as CCW and CW, corresponding to low and high kinase activity states respectively.

To assess the signalling properties of mutant Tsr molecules, we transferred *tsr* plasmids bearing HAMP lesions (derivatives of pPA114 or pRR53; see *Experimental procedures*) to host strains deleted for all chromosomal receptor genes (*tsr, tar, tap, trg, aer*) and examined their flagellar rotation patterns by cell tethering. To determine whether a receptor's output was subject to sensory adaptation control, we compared the rotation profiles of strains with and without the MCP modifying enzymes, CheB and CheR. Newly synthesized Tsr molecules have a QEQE

configuration at the four principal methylation sites (Q297, E304, Q311, E493). The Q residues are functionally similar to methylated E sites, but CheB can convert them to glutamate residues through an irreversible deamidation reaction (Kehry *et al*., 1983). The CheR methyltransferase attaches methyl groups to E residues; the CheB methylesterase hydrolyses glutamyl methyl esters, reforming glutamates (Stock and Simms, 1988). In cells lacking both CheB and CheR function, Tsr molecules retain a QEQE pattern, which mimics an intermediate methylation state (Parkinson and Houts, 1982; Kehry *et al*., 1983; Sourjik and Berg, 2002). Wild-type Tsr molecules in the QEQE state are highly kinase activating; tethered cells spend about 75% of their rotation time in the CW mode (Ames *et al*., 2008; Mowery *et al*., 2008) (Table S1 and Fig. 5). In cells containing CheB and CheR, wild-type Tsr molecules exhibit more CCW output, producing about 25% CW rotation (Ames *et al*., 2008; Mowery *et al*., 2008) (Table S1 and Fig. 5). Thus, in adaptation-proficient cells the interplay of CheB and CheR modifications adjusts receptor output to relatively low kinase activity, which represents the adaptation set point for wild-type Tsr molecules.

### *Signalling properties of Tsr-HAMP AS1 and AS2 missense mutants*

Our initial dynamic bundle model emerged from a survey of single amino acid replacements in the AS1 and AS2 helices of Tsr HAMP (Zhou *et al*., 2009). That study yielded 45 AS1 and 73 AS2 mutant proteins with wild-type expression levels that could not mediate a chemotactic response to serine in soft agar plate assays. In the present study, we investigated the motor control signals generated by these 118 mutant receptors by determining the flagellar rotation patterns they produced in adaptation-deficient [Δ*(cheRB)*] and adaptation-proficient [*(cheRB)*$^+$] hosts (Fig. 2). We defined seven mutant output categories based on quantitative properties of the rotation patterns (see *Experimental procedures*): Two locked output classes (CCW-locked, CW-locked) were refractory to CheR/CheB control; five adjustable output classes (inverted, CCW-biased, CW-biased, bipolar, unbiased) exhibited different rotation patterns in the two host strains, indicating some influence of sensory adaptation on their signalling properties.

Tsr HAMP function critically depends on hydrophobic AS1 and AS2 residues that most likely pack at the core of a four-helix bundle (Fig. 2, black and dark gray positions) (Hulko *et al*., 2006; Zhou *et al*., 2009). Replacement of one of these critical hydrophobic packing residues with a charged amino acid would probably have a substantial destabilizing effect on the HAMP bundle, whereas replacement with a neutral or small polar residue should have less drastic structural consequences. The ranking of mutant output classes in Fig. 2 reflects our judgment of the relative severity of their HAMP structural lesions, based on: (i) the location and nature of the amino acid replacement, (ii) whether the lesion was dominant in coexpression tests with wild-type Tsr and (iii) whether, in coexpression tests with a wild-type aspartate receptor (Tar), the mutant receptor regained function or jammed signalling by the heterologous receptor. In the following sections we consider the structural changes and functional properties of these HAMP mutants in the context of the dynamic bundle model of HAMP signalling.

### *CCW-locked HAMP mutants*

Counter-clockwise-locked defects comprised the most numerous mutant output class, approximately one-third (44/118) of the null mutants surveyed (Fig. 2). The majority (34/44) of the CCW-locked lesions involved proline or polar amino acid replacements at the critical hydrophobic packing residues in AS1 and AS2. Of the 10 CCW-locked lesions that were not at a critical residue position, six were proline replacements and three were charged amino acids (Fig. 2). The P221F mutant is the only exception, but, as discussed in a later section, its signalling defect is probably different from the others. Thus, structural changes that cause CCW-locked output most likely reduce helix potential (proline) or weaken helix–packing interactions, in both cases destabilizing the HAMP bundle. Accordingly, we propose that a drastically destabilized HAMP bundle locks the receptor in a kinase-off output state. The prevalence of dominant defects and the paucity of functionally rescuable ones in the CCW-locked class (see Fig. 2) support this assessment of their structural severity.

It is important to note that the CCW output produced by this group of mutant receptors does not correspond to a HAMP null condition. Tsr molecules with a complete deletion of the HAMP domain produce high CW activity, which represents the HAMP-independent, default output state of the receptor (Parkinson, 2010).

Receptor molecules that cannot generate CW output could either be defective in assembling ternary signalling complexes or they could form signalling complexes that are conformationally locked in a kinase-inactive state. To assess ternary complex formation by CCW-locked mutant receptors *in vivo*, we examined their ability to form cellular clusters observable with either of two fluorescently tagged reporter proteins, CFP-CheZ and YFP-CheR. We focused on lesions at the critical AS1 and AS2 packing residues (Fig. 3A). We first surveyed the CCW-locked receptors with a CFP-CheZ reporter, which reveals ternary signalling complexes by binding to $CheA_S$ subunits, an alternate *cheA* translation product (Smith and Parkinson, 1980; Cantwell *et al*., 2003). With this reporter, 14/24 AS1

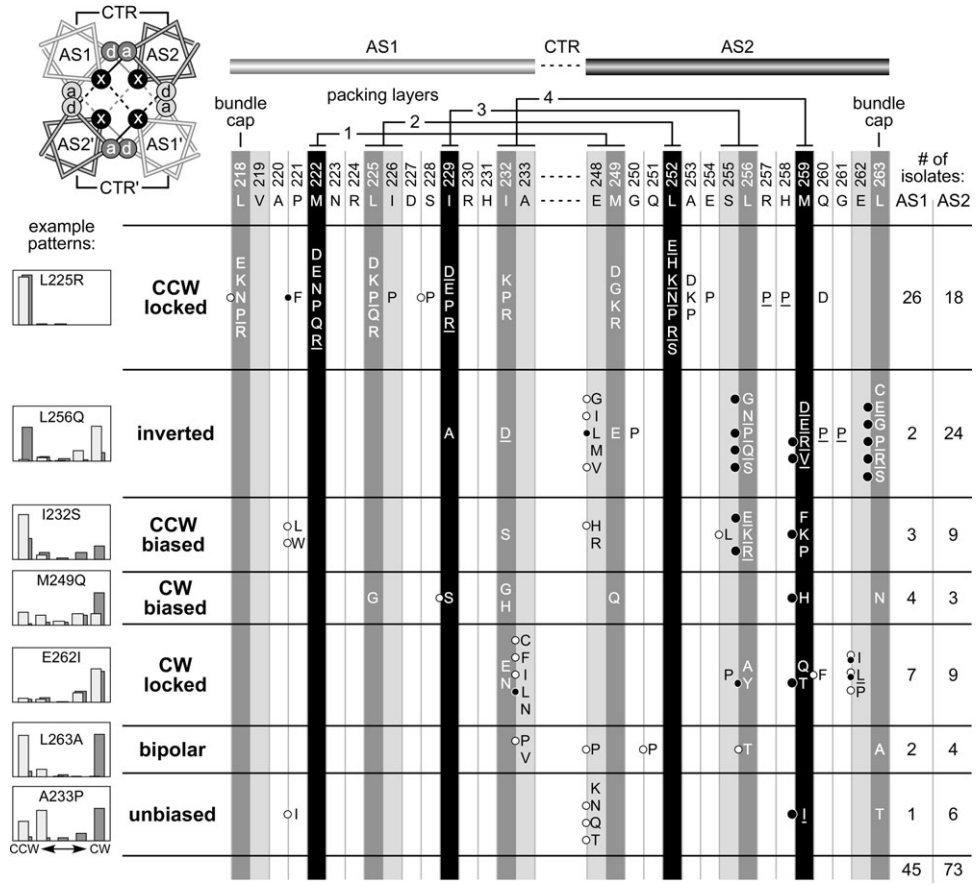


**Fig. 2.** Output patterns of Tsr molecules with null lesions in the AS1 and AS2 HAMP helices. AS1 and AS2 hydrophobic residues that are most critical for signalling function are highlighted in black and dark gray (Zhou *et al*., 2009). The residues at light gray positions are not critical for Tsr-HAMP function, with the exception of A233 and E248 (Zhou *et al*., 2009), which are highly conserved HAMP features (Dunin-Horkawicz and Lupas, 2010). The helical wheel diagram at upper left views the HAMP bundle from the N-termini of the helices and shows the packing interactions of the *x-da* arrangement: Residues at *x* positions stabilize both intrasubunit (solid lines) and intersubunit (dashed lines) interactions; the critical *a* and *d* positions (dark gray) contribute to intrasubunit interactions; the less critical *a* and *d* positions (light gray) contribute to intersubunit interactions. Two adjacent packing layers are depicted: black interaction lines for the upper layer; gray interaction lines for the lower layer. The residue interactions of the four bundle-packing layers are indicated above the AS1 and AS2 sequences. Amino acid replacements at each AS1 and AS2 residue that abrogate Tsr function are listed in single-letter designation; not all possible replacements were obtained at each position (Zhou *et al*., 2009). Underlined amino acid replacements cause dominant functional defects (Zhou *et al*., 2009). Black circles to the left of some replacements indicate lesions that jam the function of wild-type Tar receptors; larger circles denote extremely potent jammers (Zhou *et al*., 2009). White circles indicate mutant receptors that regain function in the presence of wild-type Tar receptors (Zhou *et al*., 2009). The histograms illustrate typical flagellar rotation patterns for each mutant output class, as defined in *Experimental procedures*. The heights of the histogram bars indicate the percentage of rotating cells in each of five categories, from exclusively CCW on the left to exclusively CW on the right. Host strains for the mutant Tsr plasmids were adaptation-deficient [Δ*(cheRB)*] (dark gray bars) and adaptation-proficient [*(cheRB)*$^+$] (light gray bars). This shading convention reflects the relative modification state (Q residues or methylated E residues) of wild-type receptors in the two hosts (darker represents higher modification state) and is used for rotation patterns in subsequent figures.

mutants and 10/10 AS2 mutants (Fig. 3A, plain type) formed detectable clusters (e.g. L225Q, Fig. 3B). These mutant receptors evidently assemble ternary signalling complexes that cannot activate CheA.

Ten CCW-locked AS1 mutants failed to form clusters observable with the CheZ reporter (Fig. 3A, bold type), suggesting that these receptors may not be able to assemble ternary signalling complexes. Alternatively, they might assemble ternary complexes, but fail to organize them into macroscopic clusters. To assess clustering ability directly, we tested these mutant receptors with a YFP-CheR reporter, which binds to a pentapeptide sequence at the C-terminus of the Tsr molecule (Wu *et al*., 1996; Shiomi *et al*., 2002) (see Fig. 1A). All mutant receptors that failed to form clusters with the CheZ reporter also failed to form clusters observable with the CheR reporter (e.g. M222E, Fig. 3B). It follows that these receptor mutants may have defects in an early step of ternary complex and cluster assembly, possibly in the formation of trimers of dimers, which appear to be structural precur-

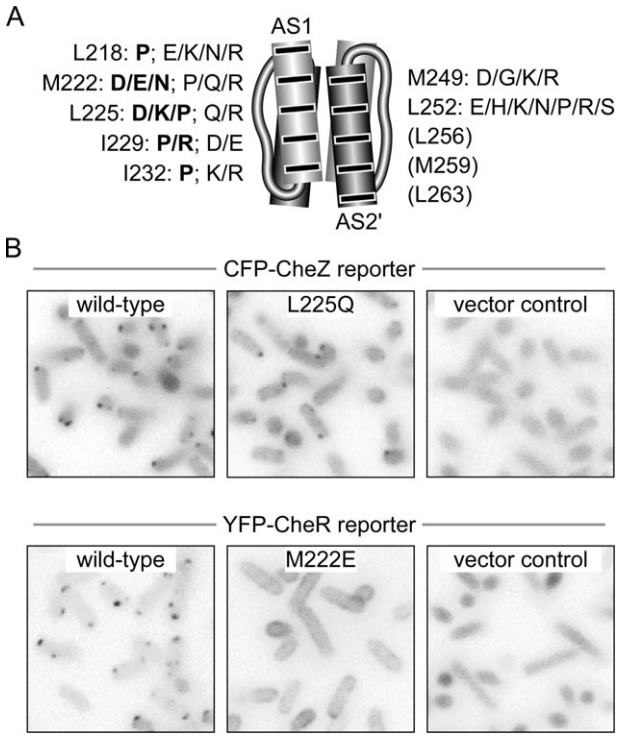


**Fig. 3.** Clustering properties of Tsr-HAMP missense mutants with locked kinase-off outputs.
A. Amino acid replacements at critical hydrophobic AS1 and AS2 residues that cause CCW-locked outputs. Bold lettering denotes replacements that disrupt cluster formation. No lesions at residues L256, M259 or L263 produced a locked CCW phenotype.
B. Fluorescence microscopy assays for receptor clustering. The original colour images were converted to grayscale, inverted and adjusted for exposure differences. L225Q exemplifies the behaviour of a cluster-proficient mutant receptor with the CFP-CheZ reporter; M222E exemplifies the behaviour of a cluster-deficient mutant receptor with the YFP-CheR reporter.

sors of both signalling complexes and clusters (Ames *et al*., 2002; Studdert and Parkinson, 2004).

Non-clustering CCW-locked lesions were only found in the AS1 helix and included four of the five proline replacements at critical AS1 packing residues (Fig. 3A). In contrast, the CCW-locked lesions that allowed ternary complex formation included a glycine replacement (M249G) and polar, but uncharged, amino acid replacements (N, Q, S) at bundle-packing residues (Fig. 3A). These distinctions suggest that the non-clustering CCW lesions cause more drastic reductions in HAMP stability than do those that retain clustering ability. We conclude that an extremely unstable HAMP bundle prevents the receptor from assembling trimers and/or ternary signalling complexes, whereas less drastically destabilized bundles allow assembly of signalling complexes, but lock them in a kinase-off state.

The distribution of CCW-locked lesions provides an important clue to their possible mechanism of kinase inactivation: We found no such lesions at any of the three C-terminal hydrophobic residues of the AS2 helix (L256, M259, L263) (Figs 2 and 3A). Although proline and charged amino acids replacements at these critical positions abrogated Tsr function, none of them caused a CCW-locked phenotype (Fig. 2). Rather, proline and charged replacements at L256, M259 and L263 caused adjustable output patterns that were inverted or CCW-biased (Fig. 2). This finding suggests that the hydrophobic residues in the C-terminal portion of AS2, hereafter designated the AS2c segment, might play instrumental roles in producing locked CCW output.

### *CW-locked and CW-biased HAMP mutants*

Over the normal physiological operating range, the dynamic bundle model predicts that reduced stability of the HAMP bundle should increase CW signal output (Fig. 1C). We found 15 CW-locked mutants and 7 CW-biased mutants, in total half the number of CCW-locked defects (Fig. 2). The lower yield of CW mutants implies that they involve more specific HAMP structural changes than do CCW-locked mutants. Indeed, CW-locked lesions only occurred at a few HAMP positions: the I232 and A233 residues at the C-terminus of AS1 and five residues in AS2c (Fig. 2). Similarly, all but one (M249Q) of the CW-biased lesions fell in the C-terminal half of AS1 or AS2 (Fig. 2). The amino acid replacements in CW mutants appear to be less destabilizing than those in CCW-locked mutants. CW lesions included glycine or serine replacements at critical AS1 hydrophobic positions (L225, I229 and I232), larger non-polar amino acids (V, L, etc.) at A233, and polar, but uncharged replacements (Q, T, N) at critical AS2 hydrophobic positions (M249, M259, L263) (Fig. 2). These CW-enhancing structural changes would no doubt weaken packing interactions between the HAMP helices, but should be less bundle-destabilizing than the charged amino acid or proline replacements in CCW-locked mutants. Consistent with this assessment, more than one-third (8/23) of the CW-locked or -biased lesions were functionally rescuable by the Tar receptor (Fig. 2).

### *Phenotypic interactions of CW and CCW lesions*

We assessed the relative structural severities of CCW-locked and CW-locked or -biased lesions by characterizing the rotation patterns produced by doubly mutant receptors. If CCW-locked defects are more bundle-destabilizing than CW lesions, CCW lesions should be epistatic to CW lesions and mutant receptors containing both types of lesions should exhibit CCW output. For CW lesions in AS1, the rotation patterns of doubly mutant receptors were consistent with this prediction (Fig. 4A).

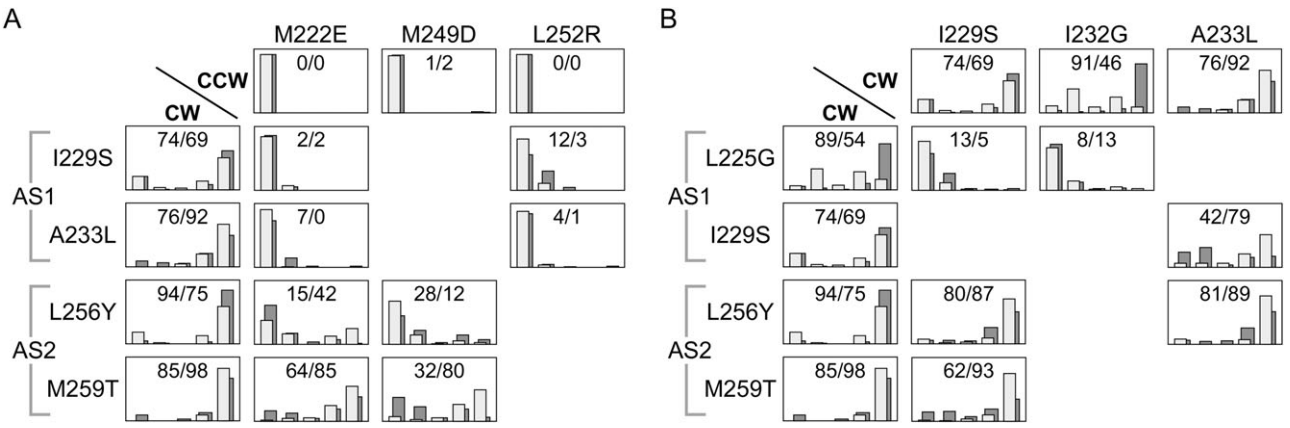


**Fig. 4.** Phenotypic interactions of Tsr-HAMP lesions that cause CCW or CW output.
A. Rotation patterns of adaptation-proficient (light gray bars) and adaptation-deficient (dark gray bars) cells expressing doubly mutant receptors with a CW and a CCW lesion. Values inside each histogram panel indicate the percent of time spent in CW rotation in the *Δ(cheRB)* strain (first value) and in the *(cheRB)*$^+$ strains (second value). Rotation classes are arranged as in Fig. 2, with exclusively CCW rotation at the left and exclusively CW rotation at the right.
B. Rotation patterns of cells expressing doubly mutant receptors with two CW lesions. Shading conventions and values are described in panel (A).

Two CW-locked lesions (I229S, A233L), when combined with a CCW-locked lesion in either AS1 (M222E) or AS2 (L252R), exhibited CCW-locked outputs (less than 15% CW in both hosts; Fig. 4A). CW-locked lesions in AS2c (L256Y, M259T) interacted in more additive fashion with CCW lesions in AS1 (M222E) and AS2 (M249D). All four of these double mutants exhibited adaptation-responsive outputs (Fig. 4A). Three (L256Y/M222E; M259T/M222E; M259T/M249D) had inverted output patterns; the fourth (L256Y/M249D) had a CCW-biased pattern (Fig. 4A).

A possible structural basis for the different behaviours of AS1 and AS2 CW lesions is suggested by the fact that AS2c hydrophobic residues seem to be critical for producing CCW-locked output. Thus, CW lesions at those residues would not produce CCW output when combined with CCW-locked lesions elsewhere in HAMP. We note that a majority of inverted and CCW-biased single mutants (24/38) have amino acid replacements in AS2c residues and that those lesions include proline and charged replacements that should drastically destabilize the HAMP bundle (Fig. 2). Conceivably, CW-locked lesions in AS2c both reduce stability of the HAMP bundle and damage the signalling structure responsible for CCW-locked output. The interaction of those two structural defects could trap receptors with CW-locked AS2c lesions in intermediate stability states that are largely refractory to the destabilizing effects of CCW-locked lesions.

Our working model also predicts that the bundle-destabilizing effects of CW lesions might interact additively, resulting in higher CCW output in double mutants through further destabilization of the HAMP bundle. The rotation patterns of double mutants with two CW mutations were consistent with this prediction and with the relative structural severity rankings of the mutant output classes in Fig. 2. For example, combination of L225G, a CW-biased lesion in AS1, with a second CW lesion in AS1 (I229S, I223G) resulted in CCW-locked output (Fig. 4B). Similarly, an I229S/A233L double, containing two CW-locked AS1 lesions, exhibited a CCW-biased output pattern (Fig. 4B). In contrast, double mutants containing a CW-locked lesion in AS1 (I229S, A233L) and in AS2c (L256Y, M259T) exhibited CW-locked (L256Y/I229S; L256Y/A233L) or CW-biased (M259T/I229S) output patterns, consistent with the expectation (discussed above) that CW AS2c lesions should be relatively insensitive to additional bundle-destabilizing effects (Fig. 4B).

### *Biphasic output control by the dynamic HAMP bundle*

The dynamic bundle model proposes that attractant stimuli elicit CCW motor responses by augmenting HAMP structural stability, thereby reducing the packing stability of the methylation bundle helices and deactivating CheA (Fig. 1C). We designate this kinase-off signalling state as the CCW(A) state. The sensory adaptation system opposes the CCW(A) state through CheR-mediated methylation increases that restore kinase activity (Goy *et al.*, 1977; Parkinson and Revello, 1978). Both stimulus response and subsequent adaptation occur in stable ternary signalling complexes (Gegner *et al.*, 1992; Erbse and Falke, 2009). By contrast, lesions that severely destabilize the HAMP bundle drive output to a kinase-off state that is fundamentally different from the one elicited by an attractant stimulus. CCW-locked outputs generated by structural disruptions of the HAMP bundle were not subject to sensory adaptation control and some defects of

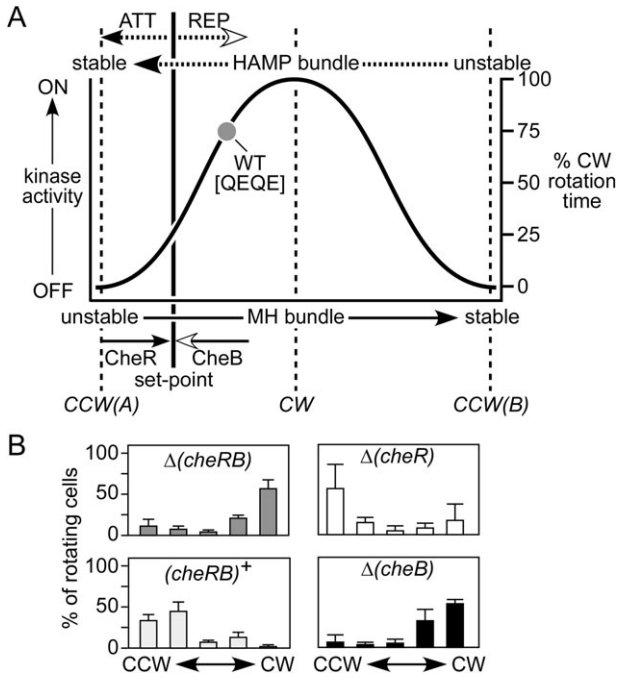


**Fig. 5.** Biphasic output diagram for Tsr-HAMP signalling.
A. The diagram summarizes the proposed relationship between HAMP or MH bundle stability and kinase activity or flagellar rotation pattern. This extended dynamic bundle model proposes two kinase-off signalling states, CCW(A) and CCW(B), at opposite extremes of the HAMP bundle stability range. Receptors with intermediate stabilities activate the CheA kinase to produce CW output signals. Wild-type Tsr molecules normally operate in the high HAMP/low MH stability regime, where kinase activity increases monotonically with HAMP instability (or MH bundle stability). The precise shape of the output curve is arbitrary. Wild-type Tsr molecules in the QEQE modification state (i.e. in adaptation-deficient strains) exhibit ~ 75% CW output (dark gray circle), which is reduced to ~ 25% CW output in adaptation-proficient strains (the adaptation set point). Filled arrowheads denote structure stabilizing influences; open arrowheads denote structure destabilizing influences. Attractant and repellent stimuli directly influence HAMP bundle stability; CheR and CheB modifications directly modulate MH bundle stability.
B. Rotation patterns produced by Tsr wild-type molecules in various strains. The rotation data are averages and standard deviations for at least three experiments (see Table S1).

this type abrogated ternary complex formation. We designate this kinase-off condition as the CCW(B) state. In summary, Tsr seems to be capable of two distinctly different kinase-off signalling states: CCW(A) is generated through attractant-induced stabilization of the HAMP bundle, whereas CCW(B) arises through drastic destabilization of the bundle and depends on hydrophobic residues at the C-terminus of the AS2 helix. This dual kinase-off logic produces a biphasic relationship between HAMP bundle stability and kinase activity (Fig. 5).

Most HAMP lesions that abrogate Tsr function probably destabilize the bundle to various extents, driving the receptor away from the adaptation set point and outside the physiological operating range (Fig. 5A). In addition to the CW and CCW(B) lesions discussed above, the biphasic model predicts the existence of destabilizing HAMP lesions that produce bundle stabilities intermediate to those of locked kinase-on and kinase-off mutants. Another HAMP signalling defect predicted by the biphasic model is a structural change that enhances bundle stability, mimicking the effects of an attractant stimulus to drive the system towards the CCW(A) kinase-off state.

To look for such mutants among the adjustable output signalling classes, we examined the rotation patterns produced by mutant receptors in hosts having only one of the two adaptation enzymes, CheB or CheR. We reasoned that any output change in either single-enzyme host relative to a host lacking both CheR and CheB must be due to action of the one enzyme present. Thus, the rotation patterns of the single-enzyme hosts can determine whether and how a mutant receptor's output responds to CheB-mediated deamidation or to CheR-mediated methylation. The rotation patterns produced by wild-type Tsr in the two single-enzyme hosts illustrate the logic of this experimental approach (Fig. 5). Wild-type Tsr produces high CW output in the QEQE modification state (Fig. 5B; gray circle in Fig. 5A). In a fully adaptation-proficient host with both CheR and CheB, Tsr CW output is reduced to the adaptation set point (Fig. 5A). The very low CW output of wild-type Tsr in the CheB-only host, and the negligible change of CW output in the CheR-only host, demonstrate that CheB deamidation is largely responsible for the CW output drop in the adaptation-proficient host (Fig. 5B). In interpreting experiments with mutant receptors, we make the assumption that, as for wild-type receptors, CheR action enhances MH bundle stability, whereas CheB action reduces MH bundle stability. For reasons that we do not yet understand, rotation patterns in the CheB-only strain were more variable than in other strains, but did not preclude a robust interpretation of the mutant output behaviours.

### *Attractant-mimic HAMP mutants*

Owing to their gain of function nature, attractant-mimic lesions could be relatively rare. Moreover, their signalling behaviour might be subject to sensory adaptation control and, consequently, such mutants could have superficially normal output patterns. Indeed, only a few HAMP null mutants exhibited normal (unbiased) or near normal (bipolar) output patterns (Fig. 2). Five of these mutants had amino acid replacements at E248, a conserved HAMP residue at the start of the AS2 helix. The rotation patterns produced by two of these mutants, E248P (bipolar) and E248K (unbiased), were suggestive of an attractant-mimic defect. Like the wild type, both mutant receptors had high CW output in the adaptation-deficient and CheR-only hosts. However, unlike the wild type, both

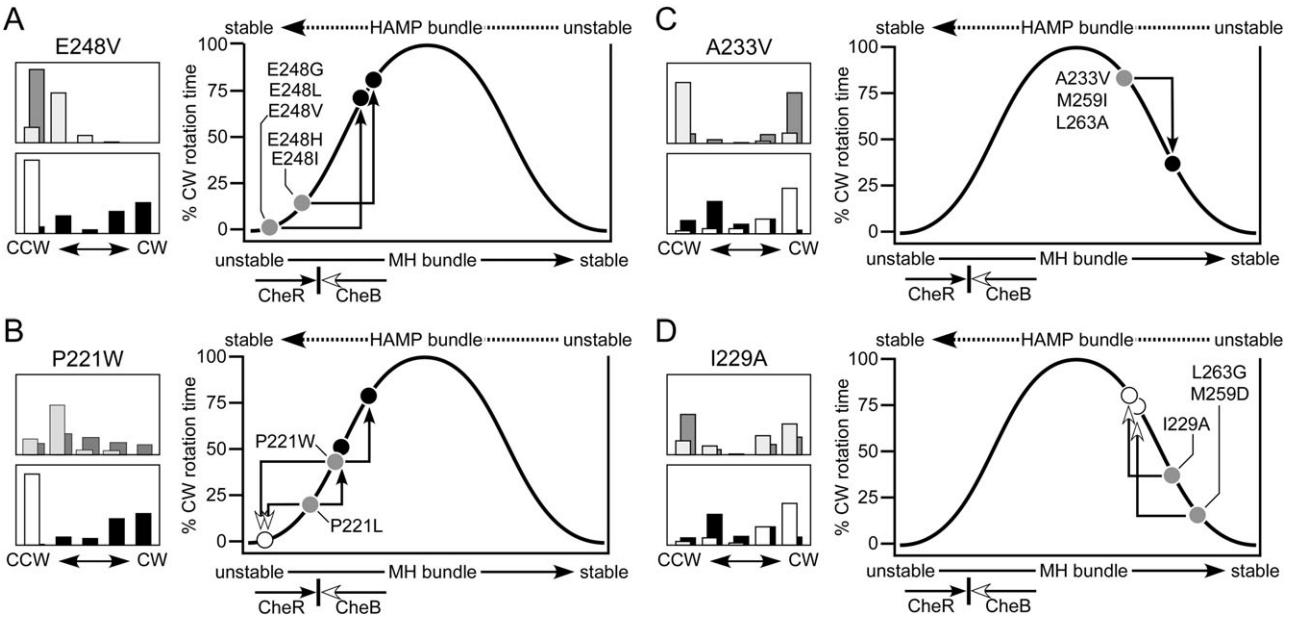


**Fig. 6.** Tsr-HAMP lesions that cause attractant-mimic and reversed response output patterns.
A. Rotation patterns for cells expressing the Tsr-E248V receptor. The upper histogram shows patterns in *Δ(cheRB)* (dark gray bars) and *(cheRB)*$^+$ (light gray bars) hosts. The lower histogram shows patterns in *Δ(cheR) cheB*$^+$ (white bars) and in *Δ(cheB) cheR*$^+$ (black bars) hosts. At right is a biphasic output diagram for E248V and for four other E248 lesions that cause similar signalling behaviour (see Table S4). Their low CW output in the QEQE state (dark gray circles) is greatly enhanced by CheR (black circles) and unaffected by CheB.
B. Rotation patterns for cells expressing the Tsr-P221W receptor. The hosts and shading conventions are described in panel (A). At right is a biphasic output diagram for P221W and for the P221L lesion, which causes similar signalling behaviour (see Table S4). Their intermediate CW outputs in the QEQE state (dark gray circles) are reduced by CheB (white circle), and increased by CheR (black circles).
C. Rotation patterns for cells expressing the Tsr-A233V receptor. The hosts and shading conventions are described panel (A). At right is a biphasic output diagram for A233V and for two other HAMP lesions with similar signalling behaviour (see Table S4). Their high CW outputs in the QEQE state (dark gray circle) are substantially reduced by CheR (black circle), but relatively unchanged by CheB.
D. Rotation patterns for cells expressing the Tsr-I229A receptor. The hosts and shading conventions are described in panel (A). At right is a biphasic output diagram for I229A and for two other HAMP lesions that cause similar signalling behaviour (see Table S4). Their low CW outputs in the QEQE state (dark gray circles) are enhanced by CheB (white circles), but relatively unchanged by CheR.

were driven to fully CCW output by the CheB-only host (Table S4). Although these E248 lesions do not discernibly alter receptor output in the QEQE modification state, deamidation appears to more readily drive them towards the CCW(A) state, consistent with structural changes that have modest stabilizing effects on the HAMP bundle. The E248N, E248Q and E248T lesions (unbiased output, Fig. 2) might have comparable structural consequences.

We next examined other E248 replacement mutants for evidence of attractant-mimic behaviour by testing their rotation patterns in single-enzyme hosts. The E248V mutant had negligible CW output in the QEQE state, was unchanged in the CheB-only host, but produced high CW output in the CheR-only host (Fig. 6A). These results suggest that the E248V lesion stabilizes the HAMP bundle more than do the E248P and E248K lesions. Other E248 lesions in the inverted (E248G, E248I, E248L, E248M) and CCW-biased (E248H) output classes had similar signalling behaviours (Fig. 6A). Interestingly, most E248 mutant receptors are functionally rescuable (Fig. 2), suggesting that structural interactions with heterologous receptors, presumably in mixed trimers of dimers (Ames and Parkinson, 2006; Ames *et al*., 2008; Mowery *et al*., 2008; Zhou *et al*., 2009) can remedy their stability changes and signalling defects.

Two CCW-biased lesions at P221, a conserved HAMP residue near the start of the AS1 helix, also appeared to confer attractant-mimic properties. The P221W receptor, for example, had somewhat less CW output in the QEQE state than did wild-type Tsr (Fig. 6B). In the CheR-only host, P221W had considerably higher CW output, and in the CheB-only host considerably lower CW output (Fig. 6B). These signalling behaviours place the P221W receptor in the normal operating range, but shifted partway towards the attractant-stimulated state. The P221L receptor exhibited similar signalling properties (Fig. 6B). The P221I receptor (unbiased output, Fig. 2) was not explicitly tested, but may also have an attractant-mimic defect. We note that the P221I, P221L and P221W defects are functionally rescuable, which could be a hallmark of attractant-mimic defects. P221F, which causes locked CCW output and jamming behaviour, might represent a more extreme example of an attractant-mimic lesion. This is the only lesion in the CCW-locked class that

does not seem to cause a drastic bundle-destabilizing structural change.

*Reversed control response HAMP mutants*

HAMP lesions that drive bundle stability into the range between that of CW and CCW(B) mutants might exhibit reversed responses to adaptational modifications (Fig. 5). We looked for such mutants among the bipolar and inverted output classes (Fig. 2). Two bipolar mutants (A233V, L263A) and a mutant (M259I) close to the unbiased-bipolar border (see Table S2), exhibited reversed response behaviours: In the CheB-only host, they retained high CW output, but in the CheR-only host their CW output dropped substantially (see A233V in Fig. 6C). These lesions most likely reduce HAMP stability beyond the physiological range, where methylation increases would be expected to further destabilize the HAMP bundle, reducing CW output (Fig. 6C). Some inverted mutants also exhibited reversed response behaviour, but of opposite sign (Fig. 6D). The inverted output mutant I229A, for example, had moderate CW output in the QEQE modification state. In the CheR-only host, the I229A receptor showed little change in CW output, whereas in the CheB-only host its CW output increased substantially (Fig. 6D). We conclude that the I229A lesion drives HAMP stability into a reversed response regime where CheB-mediated deamidation can shift the mutant receptor to higher CW output (Fig. 6D). The M259D and L263G lesions caused similar signalling behaviours (Fig. 6D).

## Discussion

*Receptor signalling models: static two-state versus dynamic three-state*

Two-state models propose a simple mechanism for receptor signalling: Output kinase activity reflects the relative proportions of discrete kinase-on and kinase-off conformational states. Chemoeffector stimuli and adaptational modifications shift those proportions to elicit motor responses and subsequent sensory adaptation (Bornhorst and Falke, 2001). However, structure–function relationships in Tsr-HAMP mutants suggest that receptor signalling is mechanistically more complex, with HAMP domains operating as dynamic three-state devices (Fig. 7). In our view, HAMP signalling states do not correspond to discrete conformations, but rather to ensembles of structures with similar stabilities. HAMP bundles at the two dynamic extremes, very stable and very unstable, both cause kinase-off behaviour, although by different mechanisms (see below). HAMP bundles of intermediate stability produce kinase-on behaviour, reflecting a balance between opposing kinase-off structural forces.

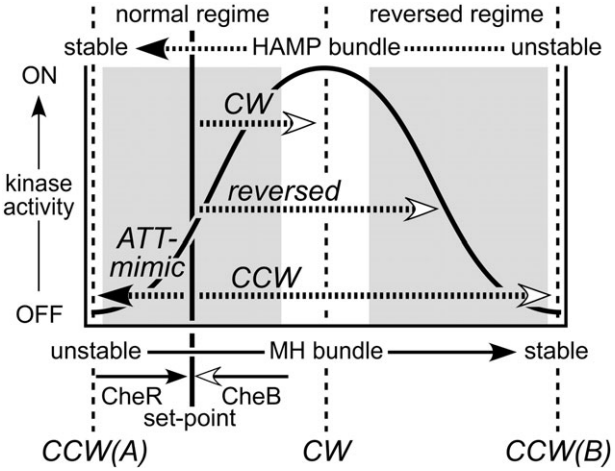


**Fig. 7.** Summary of the biphasic dynamic bundle model and mutant HAMP signalling phenotypes. This model proposes two signalling regimes (shaded areas) in which receptor output changes monotonically with HAMP stability. HAMP mutants with locked outputs are proposed to have destabilizing lesions that shift the HAMP bundle to the CW or CCW(B) portions of the stability range. Destabilizing lesions that shift HAMP into the reversed regime cause reversed output responses to CheB and CheR modification. Lesions that enhance stability of the HAMP bundle mimic the signalling effects of an attractant stimulus, shifting output towards the CCW(A) low kinase state.

The signalling properties of Tsr-HAMP mutants are difficult to reconcile with a two-state model. Assuming that most HAMP lesions are structure-destabilizing, two-state models would posit that locked output lesions damage the opposing signalling state. In contrast, the dynamic bundle model proposes that both lock-on and lock-off lesions destabilize the same structure, the HAMP bundle, but to different extents (Fig. 7). The dynamic model readily accounts for the fact that some combinations of CW defects produce CCW output and that CCW-locked defects are epistatic to some CW-locked lesions. Two-state models predict – incorrectly – that doubly mutant receptors with two CW lesions should retain CW output and that CW and CCW lesions should balance one another's output bias.

*Receptor mutants with reversed output responses*

The biphasic relationship between HAMP bundle stability and kinase activity inherent to the dynamic three-state model defines normal and reversed receptor signalling regimes. Kinase activity varies monotonically with HAMP stability in both regimes (Fig. 7). We assume that the stability consequences of adaptational modifications are the same over the entire dynamic range: Methylation stabilizes the MH bundle and consequently destabilizes the HAMP bundle; deamidation and demethylation have the

opposite effects. It follows that HAMP lesions that drive the system into the reversed regime might produce reversed signalling responses to CheB or CheR action. In fact, we found a number of Tsr-HAMP mutant receptors with such behaviour: In some, CheB action raised their CW output; in others, CheR action reduced their CW output. Two-state models cannot account for reversed signalling responses of this sort.

Several other examples of receptors with reversed signalling behaviours have been reported in the literature. The kinase activity of the NarX sensor kinase normally increases in the presence of nitrate; however, some NarX-HAMP deletions reverse the nitrate response (Appleman and Stewart, 2003; Stewart and Chen, 2010). Some mutants of the aerotaxis transducer Aer show inverted responses to oxygen stimuli (Repik *et al*., 2000). Also, Tsr-dependent aerotactic responses are reversed in cells containing CheR, but lacking CheB (Dang *et al*., 1986). Under these conditions, Tsr molecules have an abnormally high methylation state, which might drive them into the reversed response regime. In fact, Tsr molecules with methylation-mimicking Q residues at all five methylation sites have reduced CW output *in vivo* compared with those in the QEQE state (P. Ames *et al*., unpublished). These sorts of reversed responses are readily explained by the three-state, dynamic bundle model.

Tsr residue I229, near the C-terminus of the AS1 helix, plays a prominent role in the two-state gearbox model of HAMP signalling (Hulko *et al*., 2006). In Af1503 and many other HAMP domains this AS1 residue is an alanine, which Hulko *et al*. suggested should reduce bundle stability (Hulko *et al*., 2006). Indeed, an alanine replacement at Tsr-I229 produced an inverted output pattern, consistent with a destabilized HAMP bundle. However, Hulko *et al*. further suggested that larger hydrophobic residues at this HAMP position promote an alternative bundle arrangement with an opposing output state. In Tsr this is clearly not the case because both wild-type and the I229A mutant molecules elicit similar levels of kinase activity in the QEQE modification state (Fig. 6D). Their main difference lies in their response to adaptational modifications, which shift the wild-type and mutant receptor outputs in opposite directions. Perhaps signalling proteins with an alanine at this HAMP position operate in a different dynamic regime than do MCP molecules. In that case, stimuli that stabilize the HAMP bundle could enhance output activity, rather than reducing it as attractant stimuli do with chemoreceptors.

### *Structural correlates of HAMP signalling states*

The dynamic bundle model proposes that amino acid replacements in HAMP that mimic the signalling effects of attractant stimuli enhance stability of the four-helix bundle. Two conserved HAMP residues, P221 and E248, gave rise to attractant-mimic mutants. These residues abut M249 and M222 in the first packing layer of the HAMP bundle (Fig. 8A). Hydrophobic replacements at either residue shifted the receptor towards the CCW(A) signalling state, perhaps by augmenting helix–packing interactions. Conceivably, the wild-type residues at these positions poise the HAMP bundle at an intermediate stability needed for stimulus and adaptation control. P221 could serve to reduce helix potential at the N-terminus of AS1. E248, whose carboxyl group should be excluded from the hydrophobic core, could conceivably reduce packing stability of the HAMP bundle. Although some hydrophobic replacements (e.g. isoleucine) at P221 and E248 had relatively modest effects on steady-state signal output, they nevertheless abrogated stimulus responses. These control defects suggest that stimulus inputs influence packing stability at the membrane-proximal end of the HAMP bundle to modulate receptor signal output; effective control is only possible over a limited range of bundle stabilities.

A highly destabilized HAMP bundle shifts Tsr to the CCW(B) output state, which causes impaired ternary complex assembly or control. CCW(B) receptors cannot jam, or be rescued by, heterologous receptors, consistent with a defect in forming mixed trimers of dimers. Polar and charged amino acid replacements at critical packing residues in the first two layers of the HAMP bundle produced this locked, kinase-off phenotype (Fig. 8B). These structural changes should weaken or disrupt helix–packing interactions in the membrane-proximal half of the bundle. Because hydrophobic packing residues in the C-terminal half of the AS2 helix play a key role in generating this output state, it seems likely that CCW(B) signalling involves relaxation of the bundle constraints on AS2, allowing the AS2c residues to adopt an orientation or interaction that enhances packing stability of the methylation helix bundle.

A moderately destabilized HAMP bundle shifts Tsr to a locked CW output state. Only residues in the membrane-distal half of the HAMP bundle gave rise to this locked-on phenotype (Fig. 8C and D). Modest structural changes at AS2 packing residues L256 and M259 caused CW-locked output, as did polar or charged replacements at connector residue I241, whose side-chain probably contributes to bundle stability by packing between the AS1 and AS2 helices of each Tsr subunit (Fig. 8C) (Hulko *et al*., 2006; Ames *et al*., 2008). In addition, hydrophobic replacements at A233 in the C-terminus of AS1 and at AS2 residue E262, whose side-chain packs against A233, caused CW-locked behaviour (Fig. 8C). Considered together, CW-locked lesions most likely distort the packing stability or orientation of the C-terminal half of the AS2 helix.

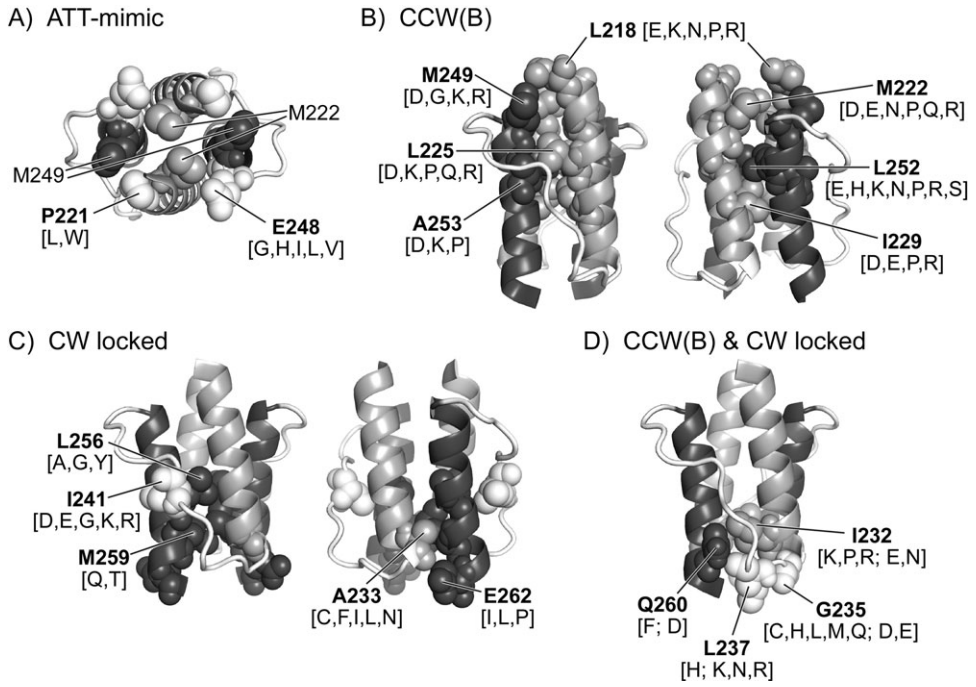


**Fig. 8.** Locations in the Tsr-HAMP bundle of lesions that cause different mutant output signals. Shading conventions in all panels: AS1, AS1' (gray); AS2, AS2' (dark gray); connector (white). Amino acid replacements (indicated in square brackets) at the residues listed in bold type produce the indicated signalling behaviour.
A. Amino acid replacements at P221 and E248 (white, spacefilled) cause attractant-mimic effects. The HAMP bundle is viewed from the N-termini of the helices. M222 (AS1) and M249 (AS2) abut P221 and E248 in the first packing layer of the HAMP bundle.
B. HAMP residues at which amino acid replacements cause CCW-locked, but not CW-locked output. Labelled residues are shown in space-filled mode in both subunits of the HAMP dimer. The N-termini of the helices are at the top of the structure.
C. HAMP residues at which amino acid replacements cause CW-locked, but not CCW-locked output. Residue I241 is in the connector segment. Signalling properties of connector lesions were described in a previous study (Ames *et al*., 2008).
D. HAMP residues at which amino acid replacements can cause either CCW- or CW-locked output. Replacements that cause CCW output are listed first; replacements listed after the semicolon cause CW output. Residues G235 and L237 lie at the beginning of the connector segment.

Residues I232, G235, L237 and Q260 in packing layer four of the HAMP bundle gave rise to both CW- and CCW-locked mutants (Fig. 8D). The side-chains of these residues pack against one another and should influence the orientation and flexibility of the AS2 helix as it emerges from the bundle. Bulky replacements (e.g. Q260F), which might be expected to distort bundle packing, caused CCW(B) output; smaller amino acids (e.g. Q260D) caused CW-locked output. Taken together, this group of output lesions supports the idea that the structural constraints on the AS2 helix as it emerges from the HAMP bundle are the primary determinant of receptor signalling state.

### *Mechanism of HAMP output control*

The dynamic bundle model proposes that helix packing in the HAMP and MH bundles is oppositionally coupled through a phase stutter at the AS2-MH1 junction (Zhou *et al*., 2009). The resultant phase clash enables HAMP domains to control receptor output by modulating the packing stability of the four-helix methylation bundle (Zhou *et al*., 2009; Parkinson, 2010). The present study provides additional insight into how this control might be accomplished (Fig. 9). We suggest that stable packing of the MH bundle, for example, at high methylation states, reduces stability of the HAMP bundle, shifting it towards the CCW(B) state. In turn, the relaxed structural constraints on the AS2c segment attenuate the phase clash, allowing AS2c hydrophobic residues to adopt a packing phase compatible with that of the MH helices, thereby contributing to stabilization of the MH bundle. The interplay of these opposing structural forces could produce a regulatable balance between the CCW(A) and CCW(B) extremes, allowing the receptor to operate across the physiological range of dynamic states.

Although the CCW(B) state is cryptic in wild-type receptors, revealed only by strongly destabilizing HAMP lesions, CCW(B) structural forces most likely contribute to HAMP function. The bundle-packing hydrophobic residues in the AS2c segment of HAMP (L256, M259, L263), which are essential for CCW(B) output, seem to play unique signalling roles. Nearly all amino acid replacements at these positions abrogate Tsr function and many

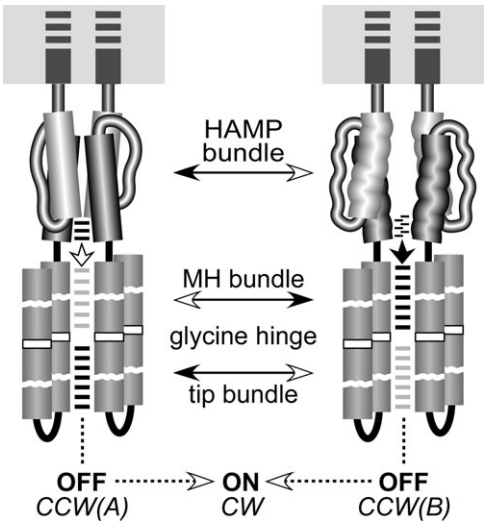


**Fig. 9.** Possible structural nature of HAMP signalling states. The membrane-spanning TM2 segments that transmit conformational signals from the periplasmic sensing domain to the AS1 helices of HAMP are shown as dark gray rectangles embedded in the cytoplasmic membrane (gray). The MH and tip bundles are not drawn to scale; see Fig. 1A for a more realistic picture of the receptor molecule. The HAMP, MH, and tip bundles appear to have opposing structural stabilities (open arrowheads indicate reduced stability; filled arrowheads indicate increased stability). A phase stutter in the AS2-MH1 connection may cause a helical phase clash between the HAMP and MH bundles (Zhou *et al*., 2009; Parkinson, 2010). The MH bundle and the tip bundle, which contains the protein interaction sites for trimer formation and ternary complex assembly, also appear to have an opposed stability relationship (Swain *et al*., 2009), which might be mediated through a flexible connecting region and glycine hinge (Coleman *et al*., 2005; Alexander and Zhulin, 2007). These structural interactions may modulate the relative strength of intrasubunit and intersubunit coiled-coil interactions in the HAMP, MH and tip bundles. Black lines between helices denote strong interactions; gray or no lines indicate weakened interactions. In the CCW(A) state, a stable HAMP bundle reduces intersubunit packing stability of the MH bundle (white arrowhead), leading to tighter packing at the receptor tip. In the CCW(B) state, a weakened HAMP bundle relaxes structural constraints on the AS2 helices, allowing an altered AS2/AS2' packing arrangement that enhances structural stability of the MH bundle (black arrowhead), leading to a highly dynamic receptor tip. A balanced interplay of these alternative structural forces poises HAMP in an intermediate stability state that allows kinase activation and CW signal output. Tsr HAMP normally operates between the CCW(A) and CW states, where modification changes in the methylation helices oppose HAMP structural forces to poise the receptor at the adaptational set point.

of those lesions probably shift HAMP stability to the reversed response regime (inverted, CCW-biased, CW-biased output patterns). Notably, most of these mutant receptors are potent jammers of heterologous receptors (Fig. 2). Functional jamming occurs in mixed trimers of dimers; the mutant members of the signalling teams block stimulus control (Ames *et al*., 2002; Ames and Parkinson, 2006). The simplest explanation for the powerful jamming action of AS2c lesions is that these residues are especially critical for controlling receptor output in response to stimulus input. These properties are consistent with the idea that pairing interactions of the AS2/AS2' helices respond to structural inputs from both the HAMP and MH bundles and adjust accordingly to modulate signal output. Evidently, very few amino acids, even other hydrophobic ones, have the requisite structural properties to function at these positions. Most AS2c replacements probably create receptors that are conformationally trapped in the reverse response regime and therefore potent jammers.

Swain *et al*. (Swain *et al*., 2009) recently presented evidence for opposed packing stabilities of the four-helix bundles in the methylation region and in the receptor tip where ternary complex assembly and kinase control occur. The intervening flexible region and glycine hinge (Coleman *et al*., 2005; Alexander and Zhulin, 2007) may mediate this oppositional control, but the coupling mechanism is unknown. One simple possibility is that changes in MH packing stability modulate the extent of supercoiling in the four-helix bundle. However, because one subunit at the receptor tip is constrained by its trimer-of-dimer binding interactions (Kim *et al*., 1999; Ames *et al*., 2002), the tip, presumably assisted by the flexible region, might act as a conformational fulcrum to reverse the stability consequences of bundle supercoiling.

These considerations suggest that the CCW(A) signalling state could enhance subunit packing at the receptor tip, which might freeze signalling complexes in a CheA-inactive conformation. In contrast, the CCW(B) state could weaken subunit interactions at the receptor tip. Increased dynamic behaviour at the receptor tip could account for the failure of CCW(B) receptors with the most extreme HAMP-destabilizing lesions to assemble ternary signalling complexes. CCW(B) receptors with somewhat less dynamic tips might form signalling complexes that cannot activate the CheA kinase because they are structurally unstable.

### *Dynamic influences on adaptational modifications*

In the normal operating regime, the steady-state modification levels of receptor molecules reflect their relative substrate properties for the CheB and CheR enzymes. Kinase-activating receptors are preferred substrates for CheB; kinase-inactivating receptors are preferred substrates for CheR. These different substrate properties could reflect different dynamic behaviours of receptor molecules. Mutant receptor molecules with locked signal outputs must either be refractory to adaptational modifications or impervious to their effects. Although we did not characterize the modification states of mutant receptors in the present study, it seems possible that the dynamic properties of CW-locked and CCW(B) receptors lie outside the preferred substrate ranges for both adap-

tation enzymes (Fig. 7). In contrast, mutant receptors in the intermediate, reversed dynamic region with adjustable signal outputs must, by definition, undergo adaptational modifications. We suggest that such HAMP lesions allow a wider range of dynamic motions than do the locked output lesions. To test this idea, we need to develop structural reporters that can more directly assess the dynamic properties of receptor molecules *in vivo*.

There is a clear disparity between HAMP lesions that block or allow adaptational control of receptor output and those that create jamming or rescuable properties. For example, AS2c lesions create potent jammers, implying a conformationally locked structure, but their signal outputs are adjustable by adaptational modification (Fig. 2). In contrast, CW-locked lesions at A233 and E262 are impervious to sensory adaptation, but are functionally rescued by heterologous receptors, implying conformational flexibility. Evidently, adaptational modifications and jamming/rescue effects operate on different aspects of receptor structure. The dynamic interactions between adjoining structural elements in receptor molecules may hold the key to understanding these sorts of signalling effects.

In summary, the signalling properties of Tsr-HAMP mutants are best explained by a three-state, dynamic control mechanism, which produces a biphasic relationship between the structural stability of the HAMP bundle and kinase activity in the receptor signalling complex. We conclude that a chemoreceptor molecule is highly dynamic and that signalling interactions between its adjacent structural elements modulate output activity by altering its dynamic behaviour.

## Experimental procedures

### *Bacterial strains*

All strains were derivatives of *E. coli* strain RP437 (Parkinson and Houts, 1982). Initial characterization of mutant output patterns used the adaptation-proficient strain UU1250 [Δ*aer-1 ygjG::Gm* Δ*tsr-7028* Δ(*tar-tap*)*5201* Δ*trg-100*] (Ames *et al*., 2002) and the adaptation-deficient strain UU1535 [Δ*aer-1* Δ(*tar-cheB*)*2234* Δ*tsr-7028* Δ*trg-100*] (Bibikov *et al*., 2004). Subsequent studies of mutant output behaviour used an isogenic set of adaptation variants: UU2610 [Δ*aer-1 ygjG::Gm* Δ(*tar-cheB*)*4346* Δ*tsr-5547* Δ*trg-4543*] (this work), UU2611 [Δ*aer-1* Δ(*tar-cheR*)*4283* Δ*tsr-5547* Δ*trg-4543*] (this work), UU2612 [Δ*aer*-1 Δ(*tar-tap*)*4530* Δ*tsr-5547* Δ*trg-4543*] (this work), and UU2632 [Δ*aer-1* Δ(*tar-tap*)*4530* Δ*cheB4345* Δ*tsr-5547* Δ*trg-4543*] (this work). In the construction of these latter strains, in-frame deletions were introduced into the chromosome by homologous recombination, using a two-step allele replacement procedure (Ames *et al*., 2008). Deletions were: *trg* (codon 3 fused to codon 544); *tsr* (codon 5 fused to codon 548); *cheB* (codon 3 fused to codon 346); *tar-tap* (codon 3 of *tar* fused to codon 531 of *tap*); *tar-cheR* (codon 3 of *tar* fused to codon 284 of *cheR*); *tar-cheB* (codon 3 of *tap* fused to codon 347 of *cheB*).

### *Plasmids*

Plasmids used were pKG116, a derivative of pACYC184 (Chang and Cohen, 1978) that confers chloramphenicol resistance and has a sodium salicylate inducible expression/cloning site (Buron-Barral *et al*., 2006), and pPA114, a relative of pKG116 that carries wild-type *tsr* under salicylate control (Ames *et al*., 2002); pRR48, a derivative of pBR322 (Bolivar *et al*., 1977) that confers ampicillin resistance and has an expression/cloning site with a *tac* promoter and an ideal (perfectly palindromic) *lac* operator under the control of a plasmid-encoded *lacI* repressor, inducible by IPTG (Studdert and Parkinson, 2005), and pRR53, a derivative of pRR48 that carries wild-type *tsr* under IPTG control (Studdert and Parkinson, 2005). Derivatives of pPA114 and pRR53 carrying HAMP missense mutations have been described (Ames *et al*., 2008; Zhou *et al*., 2009).

The plasmids used in receptor clustering assays were pVS49, a derivative of pACYC184 (Chang and Cohen, 1978) that makes a functional yellow fluorescent protein (YFP)-CheZ fusion protein under inducible arabinose control (Sourjik and Berg, 2000), pVS102, a relative of pVS49 that makes a functional YFP-CheR fusion protein under inducible arabinose control; pPA789, a relative of pRR48 that expresses a functional cyan fluorescent protein (CFP)-CheZ under inducible IPTG control (Ames and Parkinson, 2006), and pPA803, a pRR48 derivative that expresses a functional YFP-CheR fusion protein under inducible IPTG control (this work).

### *Construction of doubly mutant receptors*

Plasmid mutations were generated by QuikChange PCR mutagenesis as previously described (Ames *et al*., 2002), using a mutant template containing the first of the desired mutations and oligonucleotide primers designed to introduce the second of the desired mutations. All constructs were verified by sequencing the entire *tsr* coding region in candidate plasmids.

### *Expression levels of mutant Tsr proteins*

Tsr expression from pRR53 and pPA114 derivatives was analysed in strains UU1535 and UU2610 (to avoid multiple modification states) as described previously (Ames *et al*., 2002).

### *Receptor clustering assays*

Plasmids encoding pPA114 Tsr mutant derivatives were introduced by transformation into UU2612 cells already harbouring either pPA789 or pPA803; pRR53 Tsr mutant derivatives were introduced into UU2612 cells harbouring pVS49 or pVS102. Cells containing each pair of compatible plasmids were selected and maintained in media containing both chloramphenicol and ampicillin. Cultures for assays of polar receptor

clusters were grown at 30°C in Tryptone broth containing 50 μg ml$^{-1}$ ampicillin and 12.5 μg ml$^{-1}$ chloramphenicol. Tsr expression from pRR53 derivatives was induced with 100 μM IPTG, and YFP-CheZ (pVS49) or YFP-CheR (pVS102) with 0.005 and 0.01% (w/v) L(+)-arabinose respectively. Tsr expression from pPA114 derivatives was induced with 0.6 μM sodium salicylate, and CFP-CheZ (pPA789) or YFP-CheR (pPA803) with 100 μM IPTG. Cells at mid-exponential phase were examined by fluorescence microscopy and analysed as previously described (Ames *et al*., 2002).

### *Chemotaxis assays*

Host strains carrying Tsr expression plasmids were assessed for chemotactic ability on tryptone soft agar plates (Parkinson, 1976) containing appropriate antibiotics [ampicillin (50 μg ml$^{-1}$)] or chloramphenicol (12.5 μg ml$^{-1}$) and inducers (100 μM IPTG or 0.6 μM sodium salicylate). Plates were incubated for 7–10 h at 30°C or 32.5°C.

### *Flagellar rotation assays*

Flagellar rotation patterns of Tsr plasmid-containing cells were analysed by antibody tethering as described previously (Slocum and Parkinson, 1985). We classified cells into five categories according to their pattern of flagellar rotation: exclusively CCW, CCW reversing, balanced CCW-CW, CW reversing and exclusively CW. The fraction of CW rotation time for a population of tethered cells was computed by a weighted sum of these rotation classes, as described (Ames *et al*., 2002) (see Tables S1–4).

Seven output patterns of Tsr-HAMP mutant receptors, based on the extent of CW rotation in *Δ(cheRB)* and *(cheRB)*$^+$ hosts, were defined as follows: CCW-locked (≤ 15% CW in both hosts); CW-locked (≥ 70% CW both hosts); CW-biased [≥ 70% CW in *Δ(cheRB)* and 40–69% CW in *(cheRB)*$^+$]; bipolar [≥ 70% CW in *Δ(cheRB)* and < 20% CW in *(cheRB)*$^+$]; unbiased [≥ 70% CW in *Δ(cheRB)* and 20–40% CW in *(cheRB)*$^+$]; inverted [< 70% CW in Δ(cheRB) and an increase in CW behaviour in *(cheRB)*$^+$]; CCW-biased [< 70% CW in Δ(cheRB) and a further decrease in CW behaviour in *(cheRB)*$^+$].

### *Protein modelling and structural display*

Atomic co-ordinates for the Tsr HAMP domain were generated from the Af1503 HAMP co-ordinates (PDB accession number 2ASW) (Ames *et al*., 2008). Structure images were prepared with MacPyMOL software (http://www.pymol.org).

## Acknowledgements

Claudia Studdert (Universidad Nacional, Mar del Plata, Argentina) provided helpful comments on an earlier version of the manuscript. This work was supported by research Grant GM19559 from the National Institute of General Medical Sciences. The Protein-DNA Core Facility at the University of Utah receives support from National Cancer Institute Grant CA42014 to the Huntsman Cancer Institute.

## References

Airola, M., Watts, K.J., and Crane, B.R. (2010) Structure of concatenated HAMP domains provides a mechanism for signal transduction. *Structure* **18:** 436–448.

Alexander, R.P., and Zhulin, I.B. (2007) Evolutionary genomics reveals conserved structural determinants of signaling and adaptation in microbial chemoreceptors. *Proc Natl Acad Sci USA* **104:** 2885–2890.

Ames, P., and Parkinson, J.S. (2006) Conformational suppression of inter-receptor signaling defects. *Proc Natl Acad Sci USA* **103:** 9292–9297.

Ames, P., Studdert, C.A., Reiser, R.H., and Parkinson, J.S. (2002) Collaborative signaling by mixed chemoreceptor teams in *Escherichia coli*. *Proc Natl Acad Sci USA* **99:** 7060–7065.

Ames, P., Zhou, Q., and Parkinson, J.S. (2008) Mutational analysis of the connector segment in the HAMP domain of Tsr, the *Escherichia coli* serine chemoreceptor. *J Bacteriol* **190:** 6676–6685.

Appleman, J.A., and Stewart, V. (2003) Mutational analysis of a conserved signal-transducing element: the HAMP linker of the *Escherichia coli* nitrate sensor NarX. *J Bacteriol* **185:** 89–97.

Aravind, L., and Ponting, C.P. (1999) The cytoplasmic helical linker domain of receptor histidine kinase and methyl-accepting proteins is common to many prokaryotic signalling proteins. *FEMS Microbiol Lett* **176:** 111–116.

Barak, R., and Eisenbach, M. (1992) Correlation between phosphorylation of the chemotaxis protein CheY and its activity at the flagellar motor. *Biochemistry* **31:** 1821–1826.

Bibikov, S.I., Miller, A.C., Gosink, K.K., and Parkinson, J.S. (2004) Methylation-independent aerotaxis mediated by the *Escherichia coli* Aer protein. *J Bacteriol* **186:** 3730–3737.

Bolivar, F., Rodriguez, R., Greene, P.J., Betlach, M.C., Heyneker, H.L., and Boyer, H.W. (1977) Construction and characterization of new cloning vehicles. *Gene* **2:** 95–113.

Borkovich, K.A., and Simon, M.I. (1990) The dynamics of protein phosphorylation in bacterial chemotaxis. *Cell* **63:** 1339–1348.

Borkovich, K.A., Kaplan, N., Hess, J.F., and Simon, M.I. (1989) Transmembrane signal transduction in bacterial chemotaxis involves ligand-dependent activation of phosphate group transfer. *Proc Natl Acad Sci USA* **86:** 1208–1212.

Bornhorst, J.A., and Falke, J.J. (2001) Evidence that both ligand binding and covalent adaptation drive a two-state equilibrium in the aspartate receptor signaling complex. *J Gen Physiol* **118:** 693–710.

Buron-Barral, M., Gosink, K.K., and Parkinson, J.S. (2006) Loss- and gain-of-function mutations in the F1-HAMP region of the *Escherichia coli* aerotaxis transducer Aer. *J Bacteriol* **188:** 3477–3486.

Butler, S.L., and Falke, J.J. (1998) Cysteine and disulfide scanning reveals two amphiphilic helices in the linker region of the aspartate chemoreceptor. *Biochemistry* **37:** 10746–10756.

Cantwell, B.J., Draheim, R.R., Weart, R.B., Nguyen, C., Stewart, R.C., and Manson, M.D. (2003) CheZ phosphatase localizes to chemoreceptor patches via CheA-short. *J Bacteriol* **185:** 2354–2361.

Chang, A.C.Y., and Cohen, S.N. (1978) Construction and characterization of amplifiable multicopy DNA cloning vehicles derived from the p15A cryptic miniplasmid. *J Bacteriol* **134:** 1141–1156.

Coleman, M.D., Bass, R.B., Mehan, R.S., and Falke, J.J. (2005) Conserved glycine residues in the cytoplasmic domain of the aspartate receptor play essential roles in kinase coupling and on-off switching. *Biochemistry* **44:** 7687–7695.

Dang, C.V., Niwano, M., Ryu, J., and Taylor, B.L. (1986) Inversion of aerotactic response in *Escherichia coli* deficient in cheB protein methylesterase. *J Bacteriol* **166:** 275–280.

Dunin-Horkawicz, S., and Lupas, A.N. (2010) Comprehensive analysis of HAMP domains: implications for transmembrane signal transduction. *J Mol Biol* **397:** 1156–1174.

Erbse, A.H., and Falke, J.J. (2009) The core signaling proteins of bacterial chemotaxis assemble to form an ultrastable complex. *Biochemistry* **48:** 6975–6987.

Gegner, J.A., Graham, D.R., Roth, A.F., and Dahlquist, F.W. (1992) Assembly of an MCP receptor, CheW, and kinase CheA complex in the bacterial chemotaxis signal transduction pathway. *Cell* **70:** 975–982.

Goy, M.F., Springer, M.S., and Adler, J. (1977) Sensory transduction in *Escherichia coli*: role of a protein methylation reaction in sensory adaptation. *Proc Natl Acad Sci USA* **74:** 4964–4968.

Hazelbauer, G.L., and Lai, W.C. (2010) Bacterial chemoreceptors: providing enhanced features to two-component signaling. *Curr Opin Microbiol* **13:** 124–132.

Hazelbauer, G.L., Falke, J.J., and Parkinson, J.S. (2008) Bacterial chemoreceptors: high-performance signaling in networked arrays. *Trends Biochem Sci* **33:** 9–19.

Hess, J.F., Oosawa, K., Kaplan, N., and Simon, M.I. (1988) Phosphorylation of three proteins in the signaling pathway of bacterial chemotaxis. *Cell* **53:** 79–87.

Hulko, M., Berndt, F., Gruber, M., Linder, J.U., Truffault, V., Schultz, A., *et al*. (2006) The HAMP domain structure implies helix rotation in transmembrane signaling. *Cell* **126:** 929–940.

Kehry, M.R., Bond, M.W., Hunkapiller, M.W., and Dahlquist, F.W. (1983) Enzymatic deamidation of methyl-accepting chemotaxis proteins in *Escherichia coli* catalyzed by the *cheB* gene product. *Proc Natl Acad Sci USA* **80:** 3599–3603.

Kim, K.K., Yokota, H., and Kim, S.H. (1999) Four-helical-bundle structure of the cytoplasmic domain of a serine chemotaxis receptor. *Nature* **400:** 787–792.

Mowery, P., Ostler, J.B., and Parkinson, J.S. (2008) Different signaling roles of two conserved residues in the cytoplasmic hairpin tip of Tsr, the *Escherichia coli* serine chemoreceptor. *J Bacteriol* **190:** 8065–8074.

Parkinson, J.S. (1976) *cheA, cheB*, and *cheC* genes of *Escherichia coli* and their role in chemotaxis. *J Bacteriol* **126:** 758–770.

Parkinson, J.S. (2010) Signaling mechanisms of HAMP domains in chemoreceptors and sensor kinases. *Annu Rev Microbiol* **64:** 101–122.

Parkinson, J.S., and Houts, S.E. (1982) Isolation and behavior of *Escherichia coli* deletion mutants lacking chemotaxis functions. *J Bacteriol* **151:** 106–113.

Parkinson, J.S., and Revello, P.T. (1978) Sensory adaptation mutants of *E. coli*. *Cell* **15:** 1221–1230.

Repik, A., Rebbapragada, A., Johnson, M.S., Haznedar, J.O., Zhulin, I.B., and Taylor, B.L. (2000) PAS domain residues involved in signal transduction by the Aer redox sensor of *Escherichia coli*. *Mol Microbiol* **36:** 806–816.

Shiomi, D., Zhulin, I.B., Homma, M., and Kawagishi, I. (2002) Dual recognition of the bacterial chemoreceptor by chemotaxis-specific domains of the CheR methyltransferase. *J Biol Chem* **277:** 42325–42333.

Slocum, M.K., and Parkinson, J.S. (1985) Genetics of methyl-accepting chemotaxis proteins in *Escherichia coli*: null phenotypes of the *tar* and *tap* genes. *J Bacteriol* **163:** 586–594.

Smith, J.M., Rowsell, E.H., Shioi, J., and Taylor, B.L. (1988) Identification of a site of ATP requirement for signal processing in bacterial chemotaxis. *J Bacteriol* **170:** 2698–2704.

Smith, R.A., and Parkinson, J.S. (1980) Overlapping genes at the cheA locus of *Escherichia coli*. *Proc Natl Acad Sci USA* **77:** 5370–5374.

Sourjik, V., and Berg, H.C. (2000) Localization of components of the chemotaxis machinery of *Escherichia coli* using fluorescent protein fusions. *Mol Microbiol* **37:** 740–751.

Sourjik, V., and Berg, H.C. (2002) Receptor sensitivity in bacterial chemotaxis. *Proc Natl Acad Sci USA* **99:** 123–127.

Starrett, D.J., and Falke, J.J. (2005) Adaptation mechanism of the aspartate receptor: electrostatics of the adaptation subdomain play a key role in modulating kinase activity. *Biochemistry* **44:** 1550–1560.

Stewart, V., and Chen, L.L. (2010) The S helix mediates signal transmission as a HAMP domain coiled-coil extension in the NarX nitrate sensor from *Escherichia coli* K-12. *J Bacteriol* **192:** 734–745.

Stock, J., and Simms, S. (1988) Methylation, demethylation, and deamidation at glutamate residues in membrane chemoreceptor proteins. *Adv Exp Med Biol* **231:** 201–212.

Studdert, C.A., and Parkinson, J.S. (2004) Crosslinking snapshots of bacterial chemoreceptor squads. *Proc Natl Acad Sci USA* **101:** 2117–2122.

Studdert, C.A., and Parkinson, J.S. (2005) Insights into the organization and dynamics of bacterial chemoreceptor clusters through *in vivo* crosslinking studies. *Proc Natl Acad Sci USA* **102:** 15623–15628.

Swain, K.E., and Falke, J.J. (2007) Structure of the conserved HAMP domain in an intact, membrane-bound chemoreceptor: a disulfide mapping study. *Biochemistry* **46:** 13684–13695.

Swain, K.E., Gonzalez, M.A., and Falke, J.J. (2009) Engineered socket study of signaling through a four-helix bundle: evidence for a yin-yang mechanism in the kinase control module of the aspartate receptor. *Biochemistry* **48:** 9266–9277.

Watts, K.J., Johnson, M.S., and Taylor, B.L. (2008) Structure-function relationships in the HAMP and proximal signaling domains of the aerotaxis receptor Aer. *J Bacteriol* **190:** 2118–2127.

Welch, M., Oosawa, K., Aizawa, S.-I., and Eisenbach, M. (1993) Phosphorylation-dependent binding of a signal

molecule to the flagellar switch of bacteria. *Proc Natl Acad Sci USA* **90:** 8787–8791.
Williams, S.B., and Stewart, V. (1999) Functional similarities among two-component sensors and methyl-accepting chemotaxis proteins suggest a role for linker region amphipathic helices in transmembrane signal transduction. *Mol Microbiol* **33:** 1093–1102.
Winston, S.E., Mehan, R., and Falke, J.J. (2005) Evidence that the adaptation region of the aspartate receptor is a dynamic four-helix bundle: cysteine and disulfide scanning studies. *Biochemistry* **44:** 12655–12666.
Wu, J., Li, J., Li, G., Long, D.G., and Weis, R.M. (1996) The receptor binding site for the methyltransferase of bacterial chemotaxis is distinct from the sites of methylation. *Biochemistry* **35:** 4984–4993.
Wylie, D., Stock, A., Wong, C.Y., and Stock, J. (1988) Sensory transduction in bacterial chemotaxis involves phosphotransfer between Che proteins. *Biochem Biophys Res Commun* **151:** 891–896.
Zhou, Q., Ames, P., and Parkinson, J.S. (2009) Mutational analyses of HAMP helices suggest a dynamic bundle model of input-output signalling in chemoreceptors. *Mol Microbiol* **73:** 801–814.

## Supporting information

Additional supporting information may be found in the online version of this article.

Please note: Wiley-Blackwell are not responsible for the content or functionality of any supporting materials supplied by the authors. Any queries (other than missing material) should be directed to the corresponding author for the article.

**Table S1 - Rotation patterns of isogenic *cheRB* strains expressing wild-type Tsr receptors.**

| strain and *cheRB* genotype | rotation pattern | | | | | |
|---|---|---|---|---|---|---|
| | CCW only | CCW-rev | CCW-CW | CW-rev | CW only | **% CW** [a] |
| UU2610 [ Δ*(cheRB)* ] | 26 | 7 | 2 | 18 | 47 | **63** |
| | 15 | 15 | 4 | 24 | 42 | **66** |
| | 6 | 8 | 3 | 21 | 62 | **81** |
| | 4 | 4 | 5 | 27 | 60 | **84** |
| | 25 | 11 | 1 | 15 | 48 | **63** |
| | 13 | 11 | 9 | 22 | 45 | **69** |
| | 8 | 4 | 2 | 18 | 68 | **84** |
| | 4 | 3 | 4 | 19 | 72 | **88** |
| mean & standard deviation [b] | 13 ± 9 | 8 ± 4 | 4 ± 3 | 20 ± 4 | 55 ± 11 | **75 ± 11** |
| UU2612 [ *(cheRB)*$^+$ ] | 28 | 61 | 8 | 3 | 0 | **22** |
| | 41 | 32 | 8 | 14 | 5 | **28** |
| | 27 | 55 | 11 | 7 | 0 | **25** |
| | 33 | 45 | 5 | 15 | 2 | **27** |
| | 49 | 32 | 5 | 13 | 1 | **21** |
| | 28 | 61 | 8 | 3 | 0 | **22** |
| | 33 | 39 | 8 | 17 | 3 | **30** |
| mean & standard deviation [b] | 34 ± 8 | 46 ± 13 | 8 ± 2 | 10 ± 6 | 2 ± 2 | **25 ± 4** |
| UU2611 [ Δ*(cheR) (cheB)*$^+$ ] | 87 | 11 | 1 | 1 | 0 | **4** |
| | 80 | 20 | 0 | 0 | 0 | **5** |
| | 77 | 12 | 0 | 7 | 4 | **12** |
| | 73 | 15 | 7 | 5 | 4 | **15** |
| | 38 | 6 | 6 | 13 | 37 | **51** |
| | 14 | 24 | 17 | 17 | 28 | **55** |
| | 23 | 15 | 1 | 13 | 48 | **62** |
| mean & standard deviation [b] | 56 ± 30 | 15 ± 6 | 5 ± 6 | 8 ± 7 | 17 ± 20 | **29 ± 26** |
| UU2632 [ Δ*(cheB) (cheR)*$^+$ ] | 16 | 5 | 5 | 26 | 48 | **71** |
| | 16 | 6 | 9 | 17 | 52 | **71** |
| | 3 | 2 | 6 | 40 | 49 | **83** |
| | 0 | 2 | 0 | 40 | 58 | **89** |
| mean & standard deviation [b] | 6 ± 9 | 3 ± 2 | 5 ± 5 | 32 ± 13 | 53 ± 5 | **81 ± 9** |

[a] Percent CW time = %CW only + 0.75(%CW-reversing) + 0.5(%CCW-CW) + 0.25(%CCW-reversing).

[b] Values are rounded to the nearest whole number.

**Table S2 - Rotation patterns of cells expressing Tsr-HAMP mutant receptors.**

| | | rotation pattern in Δ*(cheRB)* host [a] | | | | | | rotation pattern in *(cheRB)*$^+$ host [b] | | | | | |
|---|---|---|---|---|---|---|---|---|---|---|---|---|---|
| residue number | mutant AA | CCW only | CCW -rev | CCW -CW | CW -rev | CW only | % **CW** [c] | CCW only | CCW -rev | CCW -CW | CW -rev | CW only | % **CW** [c] |
| L218 | E | 100 | 0 | 0 | 0 | 0 | **0** | 100 | 0 | 0 | 0 | 0 | **0** |
| | K | 100 | 0 | 0 | 0 | 0 | **0** | 96 | 0 | 0 | 0 | 4 | **4** |
| | N | 100 | 0 | 0 | 0 | 0 | **0** | 99 | 1 | 0 | 0 | 0 | **0** |
| | P | 100 | 0 | 0 | 0 | 0 | **0** | 98 | 0 | 0 | 0 | 2 | **2** |
| | R | 100 | 0 | 0 | 0 | 0 | **0** | 100 | 0 | 0 | 0 | 0 | **0** |
| P221 | F | 91 | 8 | 1 | 0 | 0 | **3** | 78 | 22 | 0 | 0 | 0 | **6** |
| | I | 6 | 1 | 5 | 29 | 59 | **84** | 24 | 67 | 8 | 1 | 0 | **22** |
| | L | 55 | 25 | 7 | 8 | 5 | **21** | 27 | 66 | 4 | 3 | 0 | **21** |
| | W | 16 | 29 | 24 | 17 | 14 | **46** | 27 | 64 | 9 | 0 | 0 | **21** |
| M222 | D | 100 | 0 | 0 | 0 | 0 | **0** | 78 | 22 | 0 | 0 | 0 | **6** |
| | E | 100 | 0 | 0 | 0 | 0 | **0** | 100 | 0 | 0 | 0 | 0 | **0** |
| | N | 100 | 0 | 0 | 0 | 0 | **0** | 100 | 0 | 0 | 0 | 0 | **0** |
| | P | 100 | 0 | 0 | 0 | 0 | **0** | 81 | 19 | 0 | 0 | 0 | **5** |
| | Q | 100 | 0 | 0 | 0 | 0 | **0** | 100 | 0 | 0 | 0 | 0 | **0** |
| | R | 98 | 0 | 0 | 0 | 2 | **2** | 100 | 0 | 0 | 0 | 0 | **0** |
| L225 | D | 96 | 4 | 0 | 0 | 0 | **1** | 97 | 0 | 0 | 0 | 3 | **3** |
| | G | 6 | 3 | 1 | 11 | 79 | **89** | 7 | 36 | 8 | 31 | 18 | **54** |
| | K | 100 | 0 | 0 | 0 | 0 | **0** | 100 | 0 | 0 | 0 | 0 | **0** |
| | P | 100 | 0 | 0 | 0 | 0 | **0** | 100 | 0 | 0 | 0 | 0 | **0** |
| | Q | 100 | 0 | 0 | 0 | 0 | **0** | 90 | 9 | 0 | 0 | 1 | **3** |
| | R | 96 | 2 | 2 | 0 | 0 | **2** | 100 | 0 | 0 | 0 | 0 | **0** |
| I226 | P | 100 | 0 | 0 | 0 | 0 | **0** | 100 | 0 | 0 | 0 | 0 | **0** |
| S228 | P | 100 | 0 | 0 | 0 | 0 | **0** | 100 | 0 | 0 | 0 | 0 | **0** |
| I229 | A | 55 | 7 | 0 | 14 | 24 | **36** | 19 | 12 | 1 | 26 | 42 | **65** |
| | D | 100 | 0 | 0 | 0 | 0 | **0** | 100 | 0 | 0 | 0 | 0 | **0** |
| | E | 100 | 0 | 0 | 0 | 0 | **0** | 100 | 0 | 0 | 0 | 0 | **0** |
| | P | 100 | 0 | 0 | 0 | 0 | **0** | 100 | 0 | 0 | 0 | 0 | **0** |
| | R | 100 | 0 | 0 | 0 | 0 | **0** | 90 | 10 | 0 | 0 | 0 | **3** |
| | S | 23 | 1 | 0 | 9 | 67 | **74** | 23 | 4 | 3 | 15 | 55 | **69** |
| I232 | D | 0 | 0 | 0 | 0 | 100 | **100** | 18 | 30 | 5 | 14 | 33 | **54** |
| | E | 4 | 16 | 9 | 40 | 31 | **70** | 2 | 10 | 11 | 19 | 58 | **80** |
| | G | 4 | 2 | 3 | 7 | 84 | **91** | 12 | 41 | 10 | 27 | 10 | **46** |
| | H | 8 | 6 | 1 | 7 | 78 | **85** | 50 | 3 | 5 | 11 | 31 | **43** |
| | K | 100 | 0 | 0 | 0 | 0 | **0** | 99 | 0 | 0 | 0 | 1 | **1** |
| | N | 2 | 3 | 8 | 23 | 64 | **86** | 4 | 11 | 7 | 28 | 50 | **77** |
| | P | 100 | 0 | 0 | 0 | 0 | **0** | 93 | 5 | 00 | 0 | 2 | **3** |
| | R | 98 | 1 | 0 | 0 | 1 | **1** | 86 | 10 | 1 | 2 | 1 | **6** |
| | S | 42 | 14 | 3 | 14 | 27 | **43** | 90 | 9 | 0 | 1 | 0 | **3** |
| A233 | C | 10 | 6 | 4 | 16 | 64 | **80** | 13 | 12 | 2 | 19 | 54 | **72** |
| | F | 7 | 2 | 1 | 19 | 71 | **86** | 18 | 0 | 2 | 14 | 66 | **78** |

| | | | | | | | | | | | | | |
|---|---|---|---|---|---|---|---|---|---|---|---|---|---|
| | I | 7 | 5 | 6 | 12 | 70 | **83** | 11 | 12 | 7 | 13 | 57 | **73** |
| | L | 10 | 7 | 7 | 23 | 53 | **76** | 0 | 0 | 5 | 22 | 73 | **92** |
| | N | 14 | 0 | 4 | 16 | 66 | **80** | 2 | 9 | 2 | 9 | 78 | **88** |
| | P | 8 | 6 | 6 | 15 | 65 | **81** | 39 | 61 | 0 | 0 | 0 | **15** |
| | V | 13 | 5 | 1 | 12 | 69 | **80** | 83 | 0 | 0 | 3 | 14 | **16** |
| | | | | | | | | | | | | | |
| E248 | G | 96 | 1 | 0 | 1 | 2 | **3** | 32 | 55 | 9 | 4 | 0 | **21** |
| | H | 68 | 12 | 2 | 8 | 10 | **20** | 40 | 52 | 4 | 2 | 0 | **17** |
| | I | 80 | 3 | 0 | 5 | 12 | **17** | 29 | 58 | 10 | 3 | 0 | **22** |
| | K | 7 | 15 | 7 | 27 | 44 | **72** | 32 | 56 | 4 | 5 | 3 | **23** |
| | L | 100 | 0 | 0 | 0 | 0 | **0** | 25 | 62 | 10 | 3 | 0 | **23** |
| | M | 99 | 1 | 0 | 0 | 0 | **0** | 40 | 49 | 14 | 07 | 0 | **25** |
| | N | 7 | 2 | 5 | 10 | 76 | **87** | 12 | 67 | 17 | 2 | 2 | **29** |
| | P | 7 | 10 | 8 | 13 | 62 | **78** | 75 | 22 | 1 | 2 | 0 | **8** |
| | Q | 6 | 6 | 6 | 13 | 69 | **83** | 16 | 56 | 20 | 7 | 1 | **30** |
| | R | 39 | 13 | 6 | 15 | 27 | **45** | 61 | 32 | 2 | 3 | 2 | **13** |
| | T | 4 | 2 | 3 | 12 | 79 | **90** | 18 | 60 | 15 | 7 | 0 | **28** |
| | V | 100 | 0 | 0 | 0 | 0 | **0** | 21 | 68 | 10 | 1 | 0 | **23** |
| M249 | D | 99 | 0 | 0 | 0 | 1 | **1** | 98 | 0 | 0 | 0 | 2 | **2** |
| | E | 71 | 8 | 2 | 11 | 8 | **19** | 35 | 11 | 4 | 16 | 34 | **51** |
| | G | 100 | 0 | 0 | 0 | 0 | **0** | 100 | 0 | 0 | 0 | 0 | **0** |
| | K | 99 | 0 | 0 | 0 | 1 | **1** | 100 | 0 | 0 | 0 | 0 | **0** |
| | Q | 3 | 6 | 6 | 20 | 65 | **85** | 26 | 20 | 8 | 23 | 23 | **49** |
| | R | 99 | 0 | 0 | 0 | 1 | **1** | 100 | 0 | 0 | 0 | 0 | **0** |
| G250 | P | 100 | 0 | 0 | 0 | 0 | **0** | 50 | 16 | 3 | 17 | 14 | **32** |
| Q251 | P | 16 | 0 | 0 | 24 | 60 | **78** | 50 | 50 | 0 | 0 | 0 | **13** |
| L252 | E | 100 | 0 | 0 | 0 | 0 | **0** | 100 | 0 | 0 | 0 | 0 | **0** |
| | H | 100 | 0 | 0 | 0 | 0 | **0** | 95 | 5 | 0 | 0 | 0 | **1** |
| | K | 100 | 0 | 0 | 0 | 0 | **0** | 96 | 0 | 0 | 0 | 4 | **4** |
| | N | 100 | 0 | 0 | 0 | 0 | **0** | 97 | 0 | 0 | 0 | 3 | **3** |
| | P | 81 | 15 | 0 | 0 | 4 | **8** | 98 | 0 | 0 | 0 | 2 | **2** |
| | R | 100 | 0 | 0 | 0 | 0 | **0** | 100 | 0 | 0 | 0 | 0 | **0** |
| | S | 100 | 0 | 0 | 0 | 0 | **0** | 95 | 0 | 0 | 0 | 5 | **5** |
| A253 | D | 100 | 0 | 0 | 0 | 0 | **0** | 99 | 0 | 0 | 0 | 1 | **1** |
| | K | 83 | 9 | 2 | 2 | 4 | **9** | 95 | 5 | 0 | 0 | 0 | **1** |
| | P | 82 | 11 | 0 | 5 | 2 | **9** | 63 | 28 | 0 | 6 | 3 | **15** |
| E254 | P | 100 | 0 | 0 | 0 | 0 | **0** | 97 | 3 | 0 | 0 | 0 | **1** |
| S255 | L | 61 | 4 | 4 | 10 | 21 | **32** | 73 | 5 | 6 | 8 | 8 | **18** |
| | P | 16 | 0 | 0 | 15 | 69 | **80** | 0 | 0 | 0 | 19 | 81 | **95** |
| L256 | A | 4 | 5 | 3 | 7 | 81 | **89** | 16 | 4 | 2 | 14 | 64 | **77** |
| | E | 38 | 25 | 7 | 18 | 12 | **35** | 91 | 7 | 0 | 2 | 0 | **3** |
| | G | 16 | 14 | 10 | 27 | 33 | **62** | 9 | 6 | 7 | 17 | 61 | **79** |
| | K | 23 | 19 | 9 | 23 | 26 | **53** | 35 | 14 | 11 | 16 | 24 | **45** |
| | N | 91 | 7 | 0 | 2 | 0 | **3** | 48 | 16 | 5 | 15 | 16 | **34** |
| | P | 31 | 20 | 0 | 23 | 26 | **48** | 32 | 9 | 1 | 21 | 37 | **56** |
| | Q | 67 | 8 | 5 | 4 | 16 | **24** | 3 | 7 | 1 | 20 | 69 | **86** |

| | | | | | | | | | | | | | |
|---|---|---|---|---|---|---|---|---|---|---|---|---|---|
| | R | 13 | 18 | 3 | 31 | 35 | **64** | 81 | 17 | 0 | 2 | 0 | **6** |
| | S | 52 | 15 | 4 | 12 | 17 | **32** | 9 | 0 | 0 | 12 | 79 | **88** |
| | T | 5 | 2 | 1 | 9 | 83 | **91** | 8 | 22 | 2 | 34 | 34 | **66** |
| | Y | 5 | 1 | 0 | 2 | 92 | **94** | 20 | 2 | 0 | 14 | 64 | **75** |
| R257 | P | 78 | 12 | 4 | 6 | 0 | **10** | 80 | 12 | 2 | 4 | 2 | **9** |
| H258 | P | 72 | 22 | 2 | 4 | 0 | **10** | 95 | 3 | 0 | 1 | 1 | **3** |
| M259 | D | 75 | 11 | 5 | 0 | 9 | **14** | 37 | 21 | 12 | 13 | 17 | **38** |
| | E | 46 | 12 | 13 | 12 | 17 | **36** | 32 | 16 | 2 | 21 | 29 | **50** |
| | F | 36 | 5 | 6 | 16 | 37 | **53** | 76 | 6 | 0 | 6 | 12 | **18** |
| | H | 13 | 1 | 4 | 20 | 62 | **79** | 45 | 7 | 2 | 10 | 36 | **46** |
| | I | 16 | 0 | 7 | 14 | 63 | **77** | 74 | 3 | 0 | 7 | 16 | **22** |
| | K | 45 | 6 | 3 | 7 | 39 | **47** | 86 | 8 | 0 | 6 | 0 | **7** |
| | P | 51 | 32 | 2 | 11 | 4 | **21** | 66 | 22 | 3 | 7 | 2 | **14** |
| | Q | 5 | 1 | 4 | 11 | 79 | **90** | 7 | 3 | 3 | 14 | 73 | **86** |
| | R | 69 | 13 | 3 | 8 | 7 | **18** | 7 | 6 | 5 | 31 | 51 | **78** |
| | T | 10 | 0 | 3 | 14 | 73 | **85** | 0 | 0 | 0 | 10 | 90 | **98** |
| | V | 34 | 3 | 10 | 15 | 38 | **55** | 7 | 0 | 0 | 12 | 81 | **90** |
| Q260 | D | 85 | 3 | 0 | 9 | 3 | **11** | 73 | 18 | 1 | 5 | 3 | **12** |
| | F | 2 | 0 | 2 | 24 | 72 | **91** | 18 | 6 | 1 | 21 | 54 | **72** |
| | P | 81 | 15 | 0 | 3 | 1 | **7** | 40 | 20 | 4 | 25 | 11 | **37** |
| G261 | P | 68 | 14 | 4 | 6 | 8 | **18** | 37 | 18 | 0 | 16 | 29 | **46** |
| E262 | I | 6 | 9 | 1 | 22 | 62 | **81** | 8 | 6 | 0 | 19 | 67 | **83** |
| | L | 8 | 8 | 4 | 24 | 56 | **78** | 18 | 7 | 0 | 17 | 58 | **73** |
| | P | 6 | 9 | 3 | 21 | 61 | **81** | 13 | 4 | 1 | 22 | 60 | **78** |
| L263 | A | 11 | 0 | 4 | 0 | 85 | **87** | 83 | 15 | 1 | 1 | 0 | **5** |
| | C | 90 | 4 | 2 | 0 | 4 | **6** | 59 | 22 | 7 | 11 | 1 | **18** |
| | E | 0 | 0 | 0 | 0 | 47 | **47** | 17 | 17 | 0 | 27 | 39 | **64** |
| | G | 76 | 9 | 4 | 1 | 10 | **15** | 7 | 9 | 0 | 36 | 48 | **77** |
| | N | 11 | 13 | 7 | 22 | 47 | **70** | 41 | 9 | 7 | 14 | 29 | **45** |
| | P | 65 | 24 | 0 | 4 | 7 | **16** | 5 | 13 | 0 | 16 | 66 | **81** |
| | R | 76 | 20 | 0 | 2 | 2 | **9** | 3 | 2 | 3 | 18 | 74 | **90** |
| | S | 43 | 35 | 1 | 9 | 12 | **28** | 6 | 9 | 13 | 22 | 50 | **75** |
| | T | 10 | 2 | 1 | 14 | 73 | **85** | 31 | 31 | 6 | 22 | 10 | **37** |

[a] Adaptation-deficient strains UU1535 or UU2610 were used. Values indicate the percentage of rotating cells in each category (see Experimental Procedures).

[b] Adaptation-proficient strains UU1250 or UU2612 were used. Values indicate the percentage of rotating cells in each category (see Experimental Procedures)

[c] Percent CW time = %CW only + 0.75(%CW-reversing) + 0.5(%CCW-CW) + 0.25(%CCW-reversing).

**Table S3 - Rotation patterns of cells expressing Tsr-HAMP doubly mutant receptors.**

| mutations | rotation pattern in Δ*(cheRB)* host [a] | | | | | | rotation pattern in *(cheRB)*$^+$ host [b] | | | | | |
|---|---|---|---|---|---|---|---|---|---|---|---|---|
| | CCW only | CCW -rev | CCW -CW | CW -rev | CW only | **% CW** [c] | CCW only | CCW -rev | CCW -CW | CW -rev | CW only | **% CW** [c] |
| **CW + CW** | | | | | | | | | | | | |
| L225G + I229S | 63 | 29 | 3 | 2 | 3 | **13** | 84 | 13 | 2 | 0 | 1 | **5** |
| L225G + I232G | 79 | 14 | 3 | 4 | 0 | **8** | 73 | 16 | 2 | 6 | 3 | **13** |
| I229S + L256Y | 6 | 6 | 5 | 28 | 55 | **80** | 8 | 2 | 3 | 10 | 77 | **87** |
| I229S + M259T | 16 | 17 | 8 | 21 | 38 | **62** | 2 | 1 | 4 | 11 | 82 | **93** |
| I229S + A233L | 26 | 34 | 4 | 17 | 19 | **42** | 7 | 7 | 7 | 23 | 56 | **79** |
| A233L + L256Y | 7 | 5 | 6 | 28 | 56 | **81** | 9 | 0 | 0 | 8 | 83 | **89** |
| **CW + CCW** | | | | | | | | | | | | |
| I229S + M222E | 94 | 6 | 0 | 0 | 0 | **2** | 92 | 8 | 0 | 0 | 0 | **2** |
| I229S + L252R | 61 | 33 | 5 | 1 | 0 | **12** | 88 | 12 | 0 | 0 | 0 | **3** |
| A233L + M222E | 80 | 16 | 2 | 0 | 2 | **7** | 99 | 1 | 0 | 0 | 0 | **0** |
| A233L + L252R | 92 | 5 | 1 | 0 | 2 | **4** | 96 | 4 | 0 | 0 | 0 | **1** |
| L256Y + M222E | 67 | 19 | 4 | 8 | 2 | **15** | 41 | 18 | 0 | 14 | 27 | **42** |
| L256Y + M249D | 49 | 24 | 3 | 16 | 8 | **28** | 74 | 16 | 1 | 6 | 3 | **12** |
| M259T + M222E | 18 | 14 | 5 | 21 | 42 | **64** | 2 | 5 | 6 | 27 | 60 | **85** |
| M259T + M249D | 41 | 25 | 6 | 21 | 7 | **32** | 8 | 3 | 6 | 29 | 54 | **80** |

[a] Adaptation-deficient strains UU1535 or UU2610 were used. Values indicate the percentage of rotating cells in each category (see Experimental Procedures).

[b] Adaptation-proficient strains UU1250 or UU2612 were used. Values indicate the percentage of rotating cells in each category (see Experimental Procedures)

[c] Percent CW time = %CW only + 0.75(%CW-reversing) + 0.5(%CCW-CW) + 0.25(%CCW-reversing).

**Table S4 - Rotation data for UU2611 and UU2632 cells expressing Tsr-HAMP mutant receptors.**

| | | rotation pattern in UU2611 host [a] | | | | | | rotation pattern in UU2632 host [b] | | | | | |
|---|---|---|---|---|---|---|---|---|---|---|---|---|---|
| residue number | mutant AA | CCW only | CCW -rev | CCW -CW | CW -rev | CW only | **% CW** [c] | CCW only | CCW -rev | CCW -CW | CW -rev | CW only | **% CW** [c] |
| I229 | A | 5 | 10 | 3 | 25 | 57 | **80** | 10 | 42 | 12 | 25 | 11 | **46** |
| A233 | V | 4 | 7 | 7 | 20 | 62 | **82** | 18 | 44 | 13 | 20 | 5 | **38** |
| E248 | G | 100 | 0 | 0 | 0 | 0 | **0** | 3 | 7 | 8 | 35 | 47 | **79** |
| E248 | H | 100 | 0 | 0 | 0 | 0 | **0** | 5 | 6 | 5 | 32 | 52 | **80** |
| E248 | I | 100 | 0 | 0 | 0 | 0 | **0** | 3 | 12 | 5 | 31 | 49 | **78** |
| E248 | K | 77 | 19 | 1 | 2 | 1 | **8** | 7 | 18 | 14 | 34 | 27 | **64** |
| E248 | L | 100 | 0 | 0 | 0 | 0 | **0** | 10 | 17 | 7 | 23 | 43 | **68** |
| E248 | P | 100 | 0 | 0 | 0 | 0 | **0** | 2 | 7 | 7 | 32 | 52 | **81** |
| E248 | V | 100 | 0 | 0 | 0 | 0 | **0** | 9 | 14 | 5 | 30 | 42 | **71** |
| M259 | D | 12 | 14 | 3 | 20 | 51 | **71** | 31 | 48 | 7 | 11 | 3 | **27** |
| M259 | I | 30 | 18 | 7 | 8 | 37 | **51** | 28 | 44 | 10 | 11 | 7 | **31** |
| L263 | A | 7 | 18 | 10 | 21 | 44 | **69** | 35 | 34 | 7 | 15 | 9 | **32** |
| L263 | G | 11 | 3 | 5 | 20 | 61 | **79** | 10 | 50 | 9 | 20 | 11 | **43** |

[a] UU2611 = Δ*(cheR) (cheB)*$^+$. Values indicate the percentage of rotating cells in each category (see Experimental Procedures).

[b] UU2632 = Δ*(cheB) (cheR)*$^+$. Values indicate the percentage of rotating cells in each category (see Experimental Procedures)

[c] Percent CW time = %CW only + 0.75(%CW-reversing) + 0.5(%CCW-CW) + 0.25(%CCW-reversing).